

**Recommendations for Chamber  
Quantification: A Report from the American  
Society of Echocardiography's Guidelines and  
Standards Committee and the Chamber  
Quantification Writing Group, Developed in  
Conjunction with the European Association  
of Echocardiography, a Branch of the  
European Society of Cardiology**

Members of the Chamber Quantification Writing Group are: Roberto M. Lang, MD, FASE, Michelle Bierig, MPH, RDCS, FASE, Richard B. Devereux, MD, Frank A. Flachskampf, MD, Elyse Foster, MD, Patricia A. Pellikka, MD, Michael H. Picard, MD, Mary J. Roman, MD, James Seward, MD, Jack S. Shanewise, MD, FASE, Scott D. Solomon, MD, Kirk T. Spencer, MD, FASE, Martin St John Sutton, MD, FASE, and William J. Stewart, MD

Quantification of cardiac chamber size, ventricular mass, and function ranks among the most clinically important and most frequently requested tasks of echocardiography. Standardization of chamber quantification has been an early concern in echocardiography and recommendations on how to measure such fundamental parameters are among the most often cited articles in the field.<sup>1,2</sup> During the last decades, echocardiographic methods and techniques have improved and expanded dramatically. Improvements in image quality have been significant, as a result of the introduction of higher-frequency transducers, har-

monic imaging, fully digital machines, left-sided contrast agents, and other technologic advancements.

Furthermore, echocardiography has become the dominant cardiac imaging technique, which, because of its portability and versatility, is now used in emergency, operating, and intensive care departments. Standardization of measurements in echocardiography has been inconsistent and less successful compared with other imaging techniques and, consequently, echocardiographic measurements are sometimes perceived as less reliable. Therefore, the American Society of Echocardiography (ASE), working together with the European Association of Echocardiography, a branch of the European Society of Cardiology, has critically reviewed the literature and updated the recommendations for quantifying cardiac chambers using echocardiography. Not all the measurements described in this article can be performed in all patients because of technical limitations. In addition, specific measurements may be clinically pertinent or conversely irrelevant in different clinic scenarios. This article reviews the technical aspects on how to perform quantitative chamber measurements and is not intended to describe the standard of care of which measurements should be performed in individual clinical studies. However, evaluation of chamber size and function is a component of every complete echocardiographic examination and these measurements may have an impact on clinical management.

From University of Chicago Hospitals, Chicago, IL (R.L., K.S.); St. Louis University Health Science Center, St. Louis MO (M.B.); Weill Medical College of Cornell University, New York, NY (R.D., M.R.); University of Erlangen, Erlangen, Germany (F.F.); University of California, San Francisco, CA (E.F.); Mayo Clinic, Rochester, Minn (P.P., J.S.); Massachusetts General Hospital, Boston, Mass (M.H.P.); Columbia University, New York, NY (J.S.S.); Brigham and Women's University, Boston, Mass (S.S.); University of Pennsylvania, Philadelphia, PA (M.S.J.S.); Cleveland Clinic Foundation, Cleveland, OH (W.S.).

Address reprint requests to the American Society of Echocardiography, 1500 Sunday Drive, Suite 102, Raleigh, NC 27607 (919) 864-7754.

J Am Soc Echocardiogr 2005;18:1440-1463.

0894-7317/\$30.00

Copyright 2005 by the American Society of Echocardiography.

Property of ASE. Reprint of these documents, beyond single use, is prohibited without prior written authorization of the ASE.

doi:10.1016/j.echo.2005.10.005

**Table 1** Elements of image acquisition and measurement for 2-dimensional quantitation

Aim	Method
Minimize translational motion	Quiet or suspended respiration (at endexpiration)
Maximize image resolution	Image at minimum depth necessary Highest possible transducer frequency Adjust gains, dynamic range, transmit, and lateral gain controls appropriately Frame rate $\geq 30/s$ Harmonic imaging B-color imaging
Avoid apical foreshortening	Steep lateral decubitus position Cut-out mattress Avoid reliance on palpable apical impulse
Maximize endocardial border	Contrast enhancement delineation
Identify end diastole and end systole	Mitral valve motion and cavity size rather than reliance on ECG

ECG, Electrocardiogram.

## GENERAL OVERVIEW

Enhancements in imaging have followed technologic improvements such as broadband transducers, harmonic imaging, and left-sided contrast agents. Nonetheless, image optimization still requires considerable expertise and attention to certain details that are specific to each view (Table 1). In general, images optimized for quantitation of one chamber may not necessarily be optimal for visualization or measurement of other cardiac structures. The position of the patient during image acquisition is important. Optimal views are usually obtained with the patient in the steep left lateral decubitus position using a cut-out mattress to permit visualization of the true apex while avoiding left ventricular (LV) foreshortening. The patient's left arm should be raised to spread the ribs. Excessive translational motion can be avoided by acquiring images during quiet respiration. If images are obtained during held end expiration, care must be taken to avoid a Valsalva maneuver, which can degrade image quality.

Digital capture and display of images on the echocardiographic system or on a workstation should optimally display images at a rate of at least 30 frames/s. In routine clinical practice a representative cardiac cycle can be used for measurement as long as the patient is in sinus rhythm. In atrial fibrillation, particularly when there is marked R-R variation, multiple beats should be used for measurements. Averaging measurements from additional cycles may be particularly useful when R-R intervals

are highly irregular. When premature atrial or ventricular contractions are present, measurements should be avoided in the postectopic beat because the length of the preceding cardiac cycle can influence ventricular volume and fiber shortening.

Harmonic imaging is now widely used in clinical laboratories to enhance images, especially in patients with poor acoustic windows. Although this technology reduces the dropout of endocardial borders, the literature suggests that there is a systemic tendency for higher measurements of LV wall thickness and mass, and smaller measurements of internal dimensions and volumes.<sup>3,4</sup> When analyzing serial studies on a given patient, differences in chamber dimension potentially attributable to imaging changes from the fundamental to the harmonic modality are probably smaller than the interobserver and intraobserver variability of these measurements. The best technique for comparing serial changes in quantitation is to display similar serial images side by side and make the same measurement on both images by the same person, at the same time.<sup>5</sup> It is important to note that most measurements presented in this manuscript are derived from fundamental imaging as normative values have not been established using harmonic imaging.

Left-sided contrast agents used for endocardial border delineation are helpful and improve measurement reproducibility for suboptimal studies and correlation with other imaging techniques. Although the use of contrast agents has been reviewed elsewhere in detail,<sup>6</sup> a few caveats regarding their use deserve mention. The mechanical index should be lowered to decrease the acoustic power of the ultrasound beam, which reduces bubble destruction. The image should be focused on the structure of interest. Excessive shadowing may be present during the initial phase of bubble transit and often the best image can be recorded several cardiac cycles after the appearance of contrast in the LV. When less than 80% of the endocardial border is adequately visualized, the use of contrast agents for endocardial border delineation is strongly recommended.<sup>7</sup> By improving visualization of the LV apex, the problem of ventricular foreshortening is reduced and correlation with other techniques improved. Contrast-enhanced images should be labeled to facilitate the reader identification of the imaging planes.

Quantitation using transesophageal echocardiography (TEE) has advantages and disadvantages compared with transthoracic echocardiography (TTE). Although visualization of many cardiac structures is improved with TEE, some differences in measurements have been found between TEE and TTE. These differences are primarily attributable to the inability to obtain from the transesophageal approach the standardized imaging planes/views used when quantifying chamber dimensions transthorac-

ically.<sup>8,9</sup> It is the recommendation of this writing group that the same range of normal values for chamber dimensions and volumes apply for both TEE and TTE. In this article, recommendations for quantification using TEE will primarily focus on acquisition of images that allow measurement of cardiac structures along imaging planes that are analogous to TTE.

In addition to describing a parameter as normal or abnormal (reference values), clinical echocardiographers most often qualify the degree of abnormality with terms such as “mildly,” “moderately,” or “severely” abnormal. Such a description allows the clinician to not only understand that the parameter is abnormal but also the degree to which their patient’s measurements deviate from normal. In addition to providing normative data it would be beneficial to standardize cutoffs for severity of abnormality across echocardiographic laboratories, such that the term “moderately abnormal” had the same implication in all laboratories. However, multiple statistical techniques exist for determining threshold values, all of which have significant limitations.<sup>10</sup>

The first approach would be to define cutoffs empirically for mild, moderate, and severe abnormalities based on SD above or below the reference limit derived from a group of healthy people. The advantage of this method is that these data readily exist for most echocardiographic parameters. However, this approach has several disadvantages. Firstly, not all echocardiographic parameters are normally distributed (or gaussian) in nature, making the use of SD questionable. Secondly, even if a particular parameter is normally distributed in control subjects, most echocardiographic parameters, when measured in the general population, have a significant asymmetric distribution in one direction (abnormally large for size or abnormally low for function parameters). Using the SD derived from healthy people leads to abnormally low cut-off values, which are inconsistent with clinical experience, as the SD inadequately represents the magnitude of asymmetry (or range of values) toward abnormality. This is the case with LV ejection fraction (EF) where 4 SD below the mean ( $64 \pm 6.5$ ) results in a cutoff for severely abnormal of 38%.

An alternative method would be to define abnormalities based on percentile values (eg, 95th, 99th) of measurements derived from a population that includes both healthy people and those with disease states.<sup>11</sup> Although these data may still not be gaussian, they account for the asymmetric distribution and range of abnormality present within the general population. The major limitation of this approach is that large enough population data sets simply do not exist for most echocardiographic variables.

**Table 2** Methods used to establish cut-off values of different echocardiographic parameters

	SD	Percentile	Risk	Expert opinion
Septal wall thickness	✓			✓
LV mass	✓		✓	
LV dimensions	✓		✓	
LV volumes	✓			
LV function linear method	✓			
Ejection fraction			✓	✓
RV dimensions	✓			
PA diameters	✓			
RV areas	✓			
RV function	✓			
LA dimensions	✓			
LA volumes	✓		✓	✓
RA dimensions	✓			

LA, Left atrial; LV, left ventricular; RA, right atrial; RV, right ventricular.

Ideally, an approach that would predict outcomes or prognosis would be preferred. That is, defining a variable as moderately deviated from normal would imply that there is a moderate risk of a particular adverse outcome for that patient. Although sufficient data linking risk and cardiac chamber sizes exist for several parameters (ie, EF, LV size, left atrial [LA] volume), risk data are lacking for many other parameters. Unfortunately, this approach continues to have several limitations. The first obstacle is how to best define risk. The cutoffs suggested for a single parameter vary broadly for the risk of death, myocardial infarction (MI), and atrial fibrillation, among others. In addition, much of the risk literature applies to specific populations (eg, post-MI, elderly), and not general cardiovascular risk readily applicable to consecutive patients studied in an echocardiography laboratory. Lastly, although having data specifically related to risk is ideal, it is not clear that this is necessary. Perhaps cardiac risk increases inherently as echocardiographic parameters become more abnormal. This has been shown for several echocardiographic parameters (LA dimension, wall thickness, LV size, and LV mass) which, when partitioned based on population estimates, demonstrated graduated risk, which is often nonlinear.<sup>11</sup>

Lastly, cut-off values may be determined from expert opinion. Although scientifically least rigorous, this method takes into account the collective experience of having read and measured tens of thousands of echocardiograms.

No single methodology could be used for all parameters. The tables of cutoffs represent a consensus of a panel of experts using a combination of the methods described above (Table 2). The consensus values are more robust for some parameters than others and future research may redefine the cut-off values. Despite the limitations, these partition values

**Table 3** Left ventricular quantification methods: Use, advantages, and limitations

Dimension/volumes	Use/advantages	Limitations
Linear		
M-mode	<ul style="list-style-type: none"> <li>- Reproducible</li> <li>- High frame rates</li> <li>- Wealth of accumulated data</li> <li>- Most representative in normally shaped ventricles</li> </ul>	<ul style="list-style-type: none"> <li>- Beam orientation frequently off axis</li> <li>- Single dimension may not be representative in distorted ventricles</li> </ul>
2D-Guided	<ul style="list-style-type: none"> <li>- Assures orientation perpendicular to ventricular long axis</li> </ul>	<ul style="list-style-type: none"> <li>- Lower frame rates than in M-mode</li> <li>- Single dimension only</li> </ul>
Volumetric		
Biplane Simpsons'	<ul style="list-style-type: none"> <li>- Corrects for shape distortions</li> <li>- Minimizes mathematic assumptions</li> </ul>	<ul style="list-style-type: none"> <li>- Apex frequently foreshortened</li> <li>- Endocardial dropout</li> <li>- Relies on only two planes</li> <li>- Few accumulated data on normal population</li> </ul>
Area length	<ul style="list-style-type: none"> <li>- Partial correction for shape distortion</li> </ul>	<ul style="list-style-type: none"> <li>- Based on mathematic assumptions</li> <li>- Few accumulated data</li> </ul>
Mass		
M-mode or 2D-guided	<ul style="list-style-type: none"> <li>- Wealth of accumulated data</li> </ul>	<ul style="list-style-type: none"> <li>- Inaccurate in ventricles with regional abnormalities</li> <li>- Beam orientation (M-mode)</li> <li>- Small errors magnified</li> <li>- Overestimates LV mass</li> </ul>
Area length	<ul style="list-style-type: none"> <li>- Allows for contribution of papillary muscles</li> </ul>	<ul style="list-style-type: none"> <li>- Insensitive to distortion in ventricular shape</li> </ul>
Truncated ellipsoid	<ul style="list-style-type: none"> <li>- More sensitive to distortions in ventricular shape</li> </ul>	<ul style="list-style-type: none"> <li>- Based on a number of mathematic assumptions</li> <li>- Minimal normal data</li> </ul>

2D, Two-dimensional; LV, left ventricular.

represent a leap toward the standardization of clinical echocardiography.

### QUANTIFICATION OF THE LV

LV dimensions, volumes, and wall thicknesses are echocardiographic measurements widely used in clinical practice and research.<sup>12,13</sup> LV size and performance are still frequently visually estimated. However, qualitative assessment of LV size and function may have significant interobserver variability and is a function of interpreter skill. Therefore, it should regularly be compared with quantitative measurements, especially when different views qualitatively suggest different degrees of LV dysfunction. Similarly, it is also important to cross-check quantitative data using the eyeball method, to avoid overemphasis on process-related measurements, which at times may depend on structures seen in a single still frame. It is important to account for the integration over time of moving structures seen in one plane, and the integration of 3-dimensional (3D) space obtained from viewing a structure in multiple orthogonal planes. Methods for quantitation of LV size, mass, and function using 2-dimensional (2D) imaging have been validated.<sup>14-17</sup>

There are distinct advantages and disadvantages to each of the accepted quantitative methods (Table 3). For example, linear LV measurements have been widely validated in the management of valvular

heart disease, but may misrepresent dilatation and dysfunction in patients with regional wall-motion abnormalities as a result of coronary artery disease. Thus, laboratories should be familiar with all available techniques and peer-review literature and should apply them on a selective basis.

### General Principles for Linear and Volumetric LV Measurements

To obtain accurate linear measurements of interventricular septal wall thickness (SWT), posterior wall thickness (PWT), and LV internal dimension, recordings should be made from the parasternal long-axis acoustic window. It is recommended that LV internal dimensions (LVIDd and LVIDs, respectively) and wall thicknesses be measured at the level of the LV minor axis, approximately at the mitral valve leaflet tips. These linear measurements can be made directly from 2D images or using 2D-targeted M-mode echocardiography.

By virtue of their high pulse rate, M-mode recordings have excellent temporal resolution and may complement 2D images in separating structures such as trabeculae adjacent to the posterior wall, false tendons on the left side of the septum, and tricuspid apparatus or moderator band on the right side of the septum from the adjacent endocardium. However, it should be recognized that even with 2D guidance, it may not be possible to align the M-mode cursor perpendicular to the long axis of the ventricle, which is mandatory to obtain a true minor-axis



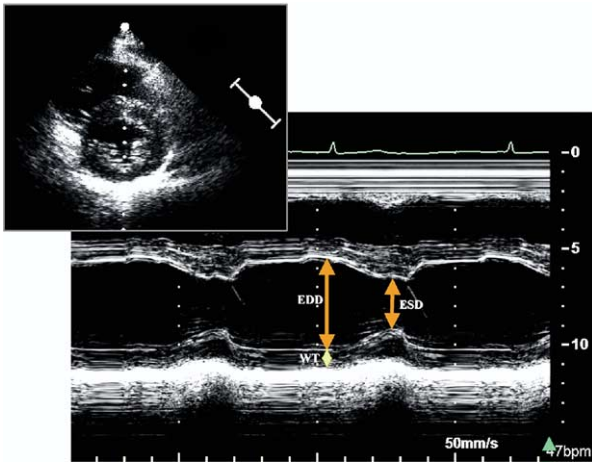


**Figure 1** Measurement of left ventricular end-diastolic diameter (EDD) and end-systolic diameter (ESD) from M-mode, guided by parasternal short-axis image (upper left) to optimize medial-lateral beam orientation.

dimension measurement. Alternatively, chamber dimension and wall thicknesses can be acquired from the parasternal short-axis view using direct 2D measurements or targeted M-mode echocardiography provided that the M-mode cursor can be positioned perpendicular to the septum and LV posterior wall.

A 2D method, useful for assessing patients with coronary artery disease, has been proposed. When using this method, it is recommended that LV internal dimensions (LVIDd and LVIDs, respectively) and wall thicknesses be measured at the level of the LV minor dimension, at the mitral chordae level. These linear measurements can also be made directly from 2D images or using 2D-targeted M-mode echocardiography. Direct 2D minor-axis measurements at the chordae level intersect the interventricular septum below the LV outflow tract<sup>2,5,18</sup> and, thus, provide a global assessment in a symmetrically contracting LV, and evaluate basal regional function in a chamber with regional wall-motion abnormalities. The direct 2D minor-axis dimensions are smaller than the M-mode measurements with the upper limits of normal of LVIDd being 5.2 versus 5.5 cm and the lower limits of normal for fractional shortening (FS) being 0.18 versus 0.25. Normal systolic and diastolic measurements reported for this parameter are  $4.7 \pm 0.4$  cm and  $3.3 \pm 0.5$  cm, respectively.<sup>2,18</sup>

LVID, SWT, and PWT are measured at end diastole and end systole from 2D or M-mode recordings,<sup>1,2</sup> preferably on several cardiac cycles (Figure 1).<sup>1,2</sup> Refinements in image processing have allowed improved resolution of cardiac structures. Consequently, it is now possible to measure the actual visualized thickness of the ventricular septum and other chamber dimensions as defined by the actual tissue-blood interface, rather than the distance between the

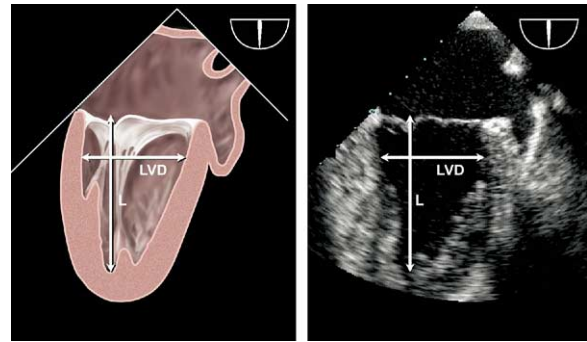


**Figure 2** Transesophageal measurements of left ventricular length (L) and minor diameter (LVD) from midesophageal 2-chamber view, usually best imaged at multiplane angle of approximately 60 to 90 degrees.

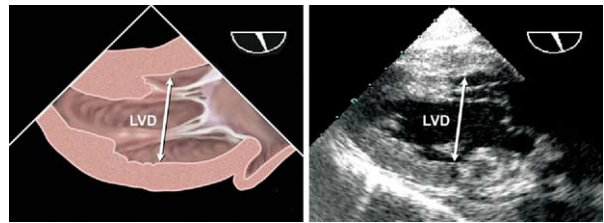


**Figure 3** Transesophageal echocardiographic measurements of left ventricular (LV) minor-axis diameter (LVD) from transgastric 2-chamber view of LV, usually best imaged at angle of approximately 90 to 110 degrees after optimizing maximum obtainable LV size by adjustment of medial-lateral rotation.

leading edge echoes, which had previously been recommended.<sup>5</sup> Use of 2D echocardiographically derived linear dimensions overcomes the common problem of oblique parasternal images resulting in overestimation of cavity and wall dimensions from M-mode. If manual calibration of images is required, 6 cm or larger distances should be used to minimize errors caused by imprecise placement of calibration points.

To obtain volumetric measurements, the most important views for 2D quantitation are the midpapillary short-axis view and the apical 4- and 2-chamber views. Volumetric measurements require manual tracing of the endocardial border. The papillary muscles should be excluded from the myocardium in the LV mass calculation (Figure 6). Accurate measurements require optimal visualization of the endocardial border to minimize the need for extrapolation. It is recommended that the basal border of the LV cavity area be delineated by a straight line connecting the mitral valve insertions at the lateral and septal borders of the annulus on the 4-chamber view and the anterior and inferior annular borders on the 2-chamber view.

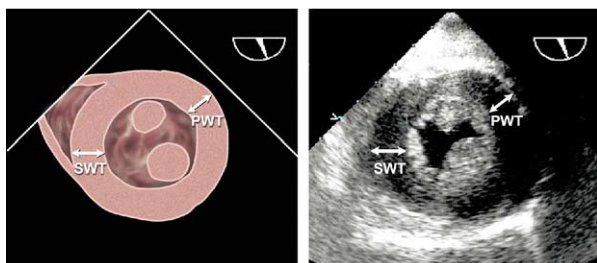


**Figure 4** Transesophageal echocardiographic measurements of wall thickness of left ventricular (LV) septal wall (SWT) and posterior wall (PWT) from transgastric short-axis view of LV, at papillary muscle level, usually best imaged at angle of approximately 0 to 30 degrees.

End diastole can be defined at the onset of the QRS, but is preferably defined as the frame after mitral valve closure or the frame in the cardiac cycle in which the cardiac dimension is largest. In sinus rhythm, this follows atrial contraction. End systole is best defined as the frame preceding mitral valve opening or the time in the cardiac cycle in which the cardiac dimension is smallest in a normal heart. In the 2-chamber view, mitral valve motion is not always clearly discernible and the frames with the largest and smallest volumes should be identified as end diastole and end systole, respectively.

The recommended TEE views for measurement of LV diameters are the midesophageal (Figure 2) and transgastric (Figure 3) 2-chamber views. LV diameters are measured from the endocardium of the anterior wall to the endocardium of the inferior wall in a line perpendicular to the long axis of the ventricle at the junction of the basal and middle thirds of the long axis. The recommended TEE view for measurement of LV wall thickness is the transgastric midshort-axis view (Figure 4). With TEE, the long-axis dimension of the LV is often foreshortened in the midesophageal 4-chamber and long-axis views; therefore, the midesophageal 2-chamber view is preferred for this measurement. Care must be made to avoid foreshortening TEE views, by recording the image plane that shows the maximum obtainable chamber size, finding the angle for diameter measurement that is perpendicular to the long axis of that chamber, then measuring the maximum obtainable short-axis diameter.

### Calculation of LV Mass

In clinical practice, LV chamber dimensions are commonly used to derive measures of LV systolic function, whereas in epidemiologic studies and treatment trials, the single largest application of echocardiography has been the estimation of LV mass in populations and its change with antihypertensive therapy.<sup>13,19</sup> All LV mass algorithms, whether using M-mode, 2D, or 3D echocardiographic measure-

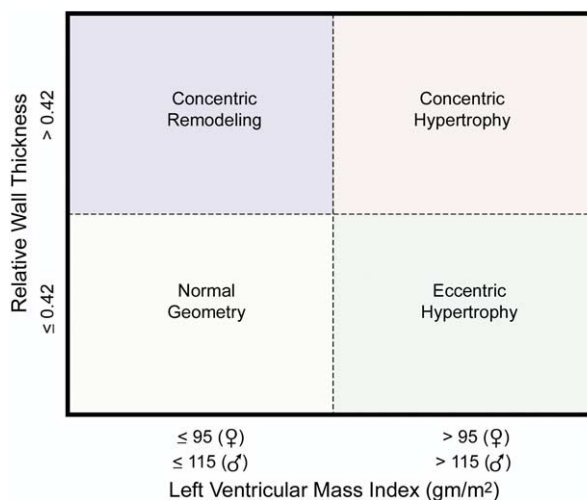


**Figure 5** Comparison of relative wall thickness (RWT). Patients with normal left ventricular (LV) mass can have either concentric remodeling (normal LV mass with increased RWT  $\geq 0.42$ ) or normal geometry (RWT  $\leq 0.42$ ) and normal LV mass. Patients with increased LV mass can have either concentric (RWT  $\geq 0.42$ ) or eccentric (RWT  $\leq 0.42$ ) hypertrophy. These LV mass measurements are based on linear measurements.

ments, are based on subtraction of the LV cavity volume from the volume enclosed by the LV epicardium to obtain LV muscle or shell volume. This shell volume is then converted to mass by multiplying by myocardial density. Hence, quantitation of LV mass requires accurate identification of interfaces between the cardiac blood pool and endocardium, and between epicardium and pericardium.

To date, most LV mass calculations have been made using linear measurements derived from 2D-targeted M-mode or, more recently, from 2D linear LV measurements.<sup>20</sup> The ASE-recommended formula for estimation of LV mass from LV linear dimensions (validated with necropsy  $r = 0.90$ ,  $P < .001$ <sup>21</sup>) is based on modeling the LV as a prolate ellipse of revolution:

$$\text{LV mass} = 0.8 \times \{1.04[(\text{LVIDd} + \text{PWTd} + \text{SWTd})^3 - (\text{LVIDd})^3]\} + 0.6 \text{ g}$$

where PWTd and SWTd are posterior wall thickness at end diastole and septal wall thickness at end diastole, respectively. This formula is appropriate for evaluating patients without major distortions of LV geometry (eg, patients with hypertension). Because this formula requires cubing primary measurements, even small errors in these measurements are magnified. Calculation of relative wall thickness (RWT) by the formula  $(2 \times \text{PWTd})/\text{LVIDd}$  permits categorization of an increase in LV mass as either concentric (RWT  $\geq 0.42$ ) or eccentric (RWT  $\leq 0.42$ ) hypertrophy and allows identification of con-

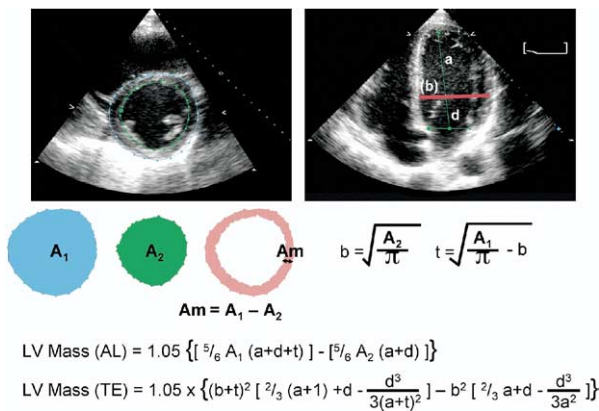


**Figure 6** Two methods for estimating LV mass based on area-length (AL) formula and the truncated ellipsoid (TE) formula, from short-axis (left) and apical four-chamber (right) 2-D echo views. Where  $A_1$  = total LV area;  $A_2$  = LV cavity area,  $A_m$  = myocardial area,  $a$  is the long or semi-major axis from widest minor axis radius to apex,  $b$  is the short-axis radius (back calculated from the short-axis cavity area) and  $d$  is the truncated semimajor axis from widest short-axis diameter to mitral anulus plane. Assuming a circular area, the radius ( $b$ ) is computed and mean wall thickness ( $t$ ) derived from the short-axis epicardial and cavity areas. See text for explanation.

centric remodeling (normal LV mass with increased RWT) (Figure 5).<sup>22</sup>

The most commonly used 2D methods for measuring LV mass are based on the area-length formula and the truncated ellipsoid model, as described in detail in the 1989 ASE document on LV quantitation.<sup>2</sup> Both methods were validated in the early 1980s in animal models and by comparing pre-mortem echocardiograms with measured LV weight at autopsy in human beings. Both methods rely on measurements of myocardial area at the midpapillary muscle level. The epicardium is traced to obtain the total area ( $A_1$ ) and the endocardium is traced to obtain the cavity area ( $A_2$ ). Myocardial area ( $A_m$ ) is computed as the difference:  $A_m = A_1 - A_2$ . Assuming a circular area, the radius is computed:  $b = \sqrt{A_2/\pi}$ , and a mean wall thickness derived (Figure 6). LV mass can be calculated by one of the two formulas shown in Figure 6. In the presence of extensive regional wall-motion abnormalities (eg, MI), the biplane Simpson's method may be used, although this method is dependent on adequate endocardial and epicardial definition of the LV, which often is challenging from this window. Most laboratories obtain the measurement at end diastole and exclude the papillary muscles in tracing the myocardial area.

TEE evaluation of LV mass is also highly accurate, but has minor systematic differences in LV PWT. In particular, LV mass derived from TEE wall-thickness measurements is higher by an average of 6 g/m<sup>2</sup>.<sup>8</sup>

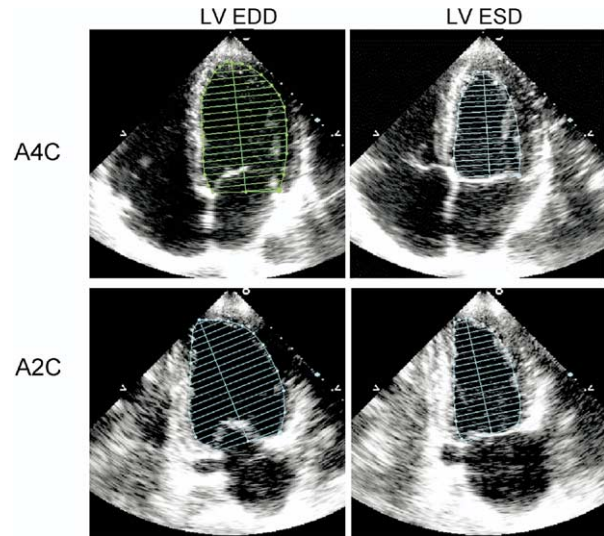


**Figure 7** Two-dimensional measurements for volume calculations using biplane method of disks (modified Simpson's rule) in apical 4-chamber (A4C) and apical 2-chamber (A2C) views at end diastole (LV EDD) and at end systole (LV ESD). Papillary muscles should be excluded from the cavity in the tracing.

**LV Systolic Function: Linear and Volumetric Measurement**

Many echocardiography laboratories rely on M-mode measurements or linear dimensions derived from the 2D image for quantification. Linear measurements from M-mode and 2D images have proven to be reproducible with low intraobserver and interobserver variability.<sup>20,23-26</sup> Although linear measures of LV function are problematic when there is a marked regional difference in function, in patients with uncomplicated hypertension, obesity, or valvular diseases, such regional differences are rare in the absence of clinically recognized MI. Hence, FS and its relationship to end-systolic stress often provide useful information in clinical studies.<sup>27</sup> The previously used Teichholz or Quinones methods of calculating LV EF from LV linear dimensions may result in inaccuracies as a result of the geometric assumptions required to convert a linear measurement to a 3D volume.<sup>28,29</sup> Accordingly, the use of linear measurements to calculate LV EF is not recommended for clinic practice.

Contraction of muscle fibers in the LV midwall may better reflect intrinsic contractility than contraction of fibers at the endocardium. Calculation of midwall rather than endocardial FS is particularly useful in revealing underlying systolic dysfunction in the setting of concentric hypertrophy.<sup>30</sup> Midwall fraction and shortening (MWFS) may be computed from linear measures of diastolic and systolic cavity sizes and wall thicknesses based on mathematic models,<sup>30,31</sup> according to the following formulas:



**Table 4** Reference limits and partition values of left ventricular mass and geometry

	Women				Men			
	Reference range	Mildly abnormal	Moderately abnormal	Severely abnormal	Reference range	Mildly abnormal	Moderately abnormal	Severely abnormal
Linear Method								
LV mass, g	67–162	163–186	187–210	≥211	88–224	225–258	259–292	≥293
<i>LV mass/BSA, g/m<sup>2</sup></i>	<i>43–95</i>	<i>96–108</i>	<i>109–121</i>	<i>≥122</i>	<i>49–115</i>	<i>116–131</i>	<i>132–148</i>	<i>≥149</i>
LV mass/height, g/m	41–99	100–115	116–128	≥129	52–126	127–144	145–162	≥163
LV mass/height <sup>2,7</sup> , g/m <sup>2,7</sup>	18–44	45–51	52–58	≥59	20–48	49–55	56–63	≥64
Relative wall thickness, cm	0.22–0.42	0.43–0.47	0.48–0.52	≥0.53	0.24–0.42	0.43–0.46	0.47–0.51	≥0.52
<i>Septal thickness, cm</i>	<i>0.6–0.9</i>	<i>1.0–1.2</i>	<i>1.3–1.5</i>	<i>≥1.6</i>	<i>0.6–1.0</i>	<i>1.1–1.3</i>	<i>1.4–1.6</i>	<i>≥1.7</i>
<i>Posterior wall thickness, cm</i>	<i>0.6–0.9</i>	<i>1.0–1.2</i>	<i>1.3–1.5</i>	<i>≥1.6</i>	<i>0.6–1.0</i>	<i>1.1–1.3</i>	<i>1.4–1.6</i>	<i>≥1.7</i>
2D Method								
LV mass, g	66–150	151–171	172–182	>193	96–200	201–227	228–254	>255
<i>LV mass/BSA, g/m<sup>2</sup></i>	<i>44–88</i>	<i>89–100</i>	<i>101–112</i>	<i>≥113</i>	<i>50–102</i>	<i>103–116</i>	<i>117–130</i>	<i>≥131</i>

BSA, Body surface area; LV, left ventricular; 2D, 2-dimensional.  
Bold italic values: Recommended and best validated.

$$\text{Inner shell} = [(LVIDd + SWTd/2 + PWTd/2)^3 - LVIDd^3 + LVIDs^3]^{1/3} - LVIDs$$

$$\text{MWFS} = \frac{[(LVIDd + SWTd/2 + PWTd/2) - (LVIDs + \text{inner shell})]}{(LVIDd + SWTd/2 + PWTd/2)} \times 100$$

The most commonly used 2D measurement for volume measurements is the biplane method of disks (modified Simpson’s rule) and is the currently recommended method of choice by consensus of this committee (Figure 7). The principle underlying this method is that the total LV volume is calculated from the summation of a stack of elliptical disks. The height of each disk is calculated as a fraction (usually 1/20) of the LV long axis based on the longer of the two lengths from the 2- and 4-chamber views. The cross-sectional area of the disk is based on the two diameters obtained from the 2- and 4-chamber views. When two adequate orthogonal views are not available, a single plane can be used and the area of the disk is then assumed to be circular. The limitations of using a single plane are greatest when extensive wall-motion abnormalities are present.

An alternative method to calculate LV volumes when apical endocardial definition precludes accurate tracing is the area-length method where the LV is assumed to be bullet-shaped. The mid-LV cross-sectional area is computed by planimetry in the parasternal short-axis view and the length of the ventricle taken from the midpoint of the annulus to the apex in the apical 4-chamber view. These measurements are repeated at end diastole and end systole, and the volume is computed according to the formula: volume = [5 (area) (length)]/6. The most widely used parameter for indexing volumes is the body surface area (BSA) in square meters.

End-diastolic volume (EDV) and end-systolic volume (ESV) are calculated by either of the two methods described above and the EF is calculated as follows:

$$\text{Ejection fraction} = (\text{EDV} - \text{ESV})/\text{EDV}$$

Partition values for recognizing depressed LV systolic function in Table 6 follow the conventional practice of using the same cutoffs in women and men; however, emerging echocardiographic and magnetic resonance imaging (MRI) data suggest that LV EF and other indices are somewhat higher in apparently healthy women than in men.<sup>32,33</sup> Quantitation of LV volumes using TEE is challenging because of difficulties in obtaining a nonforeshortened LV cavity from the esophageal approach. However, when carefully acquired, direct comparisons between TEE and TTE volumes and EF have shown minor or no significant differences.<sup>8,9</sup>

### References Values for LV Measurements

As shown in Tables 4–6, reference values for LV linear dimensions have been obtained from an ethnically diverse population of 510 normal-weight, normotensive, and nondiabetic white, African American, and American Indian adults without recognized cardiovascular disease (unpublished data). The populations from which these data have been derived have been described in detail previously.<sup>20,34–36</sup> Reference values for volumetric measurements have also been obtained in a healthy adult population.<sup>37</sup>

Normal values for LV mass differ between men and women even when indexed for BSA (Table 4). The best method for normalizing LV mass measurements in adults is still debated. Although BSA has been most often used in clinical trials, this method will underestimate the prevalence of LV hypertrophy in overweight and obese individuals. The ability to detect LV hypertrophy related to obesity and to cardiovascular diseases is enhanced by indexing LV mass for the power of its allometric or growth relation with height (height<sup>2,7</sup>). Data are inconclusive



**Table 5** Reference limits and partition values of left ventricular size

	Women				Men			
	Reference range	Mildly abnormal	Moderately abnormal	Severely abnormal	Reference range	Mildly abnormal	Moderately abnormal	Severely abnormal
LV dimension								
LV diastolic diameter	3.9–5.3	5.4–5.7	5.8–6.1	≥6.2	4.2–5.9	6.0–6.3	6.4–6.8	≥6.9
LV diastolic diameter/BSA, cm/m <sup>2</sup>	2.4–3.2	3.3–3.4	3.5–3.7	≥3.8	2.2–3.1	3.2–3.4	3.5–3.6	≥3.7
LV diastolic diameter/height, cm/m	2.5–3.2	3.3–3.4	3.5–3.6	≥3.7	2.4–3.3	3.4–3.5	3.6–3.7	≥3.8
LV volume								
LV diastolic volume, mL	56–104	105–117	118–130	≥131	67–155	156–178	179–201	≥201
<i>LV diastolic volume/BSA, mL/m<sup>2</sup></i>	<i>35–75</i>	<i>76–86</i>	<i>87–96</i>	<i>≥97</i>	<i>35–75</i>	<i>76–86</i>	<i>87–96</i>	<i>≥97</i>
LV systolic volume, mL	19–49	50–59	60–69	≥70	22–58	59–70	71–82	≥83
<i>LV systolic volume/BSA, mL/m<sup>2</sup></i>	<i>12–30</i>	<i>31–36</i>	<i>37–42</i>	<i>≥43</i>	<i>12–30</i>	<i>31–36</i>	<i>37–42</i>	<i>≥43</i>

BSA, body surface area; LV, left ventricular.

Bold italic values: Recommended and best validated.

**Table 6** Reference limits and values and partition values of left ventricular function

	Women				Men			
	Reference range	Mildly abnormal	Moderately abnormal	Severely abnormal	Reference range	Mildly abnormal	Moderately abnormal	Severely abnormal
Linear method								
Endocardial fractional shortening, %	27–45	22–26	17–21	≤16	25–43	20–24	15–19	≤14
Midwall fractional shortening, %	15–23	13–14	11–12	≤10	14–22	12–13	10–11	≤10
2D Method								
<i>Ejection fraction, %</i>	<i>≥55</i>	<i>45–54</i>	<i>30–44</i>	<i>&lt;30</i>	<i>≥55</i>	<i>45–54</i>	<i>30–44</i>	<i>&lt;30</i>

2D, Two-dimensional.

Bold italic values: Recommended and best validated.

as to whether such indexing of LV mass may improve or attenuate prediction of cardiovascular events. Of note, the reference limits for LV mass in Table 4 are lower than those published in some previous echocardiographic studies, yet are virtually identical to those based on direct necropsy measurement and cut-off values used in clinical trials.<sup>19,20,36,38,39</sup> Although some prior studies have suggested racial differences in LV mass measurement, the consensus of the literature available indicates that no significant differences exist between clinically healthy African American and Caucasian people. In contrast, a recent study has shown racial-ethnic differences in LV structure in adults with hypertension.<sup>40</sup> Although the sensitivity, specificity, and predictive value of LV wall-thickness measurements for detection of LV hypertrophy are lower than for calculated LV mass, it is sometimes easiest in clinical practice to identify LV hypertrophy by measuring an increased LV posterior and septal thickness.<sup>41</sup>

The use of LV mass in children is complicated by the need for indexing the measurement relative to patient body size. The intent of indexing is to account for normal childhood growth of lean body mass without discounting the pathologic effects of patients who are overweight or obese. In this way, an indexed LV mass measurement in early childhood can be directly compared with a subsequent mea-

surement during adolescence and adulthood. Dividing LV mass by height (meters) increased to a power of 2.5 to 3.0 is the most widely accepted indexing method in older children and adolescents because it correlates best to indexing LV mass to lean body mass.<sup>42</sup> Currently an intermediate value of 2.7 is generally used.<sup>43,44</sup> In younger children (<8 years old), the most ideal indexing factor remains an area of research, but height increased to a power of 2.0 appears to be the most appropriate.<sup>45</sup>

### Three-dimensional Assessment of Volume and Mass

Three-dimensional chamber volume and mass are incompletely characterized by 1-dimensional or 2D approaches, which are based on geometric assumptions. Although these inaccuracies have been considered inevitable and of minor clinical importance in the past, in most situations accurate measurements are required, particularly when following the course of a disease with serial examinations. During the last decade, several 3D echocardiographic techniques became available to measure LV volumes and mass.<sup>46–59</sup> These can be conceptually divided into techniques, which are based on offline reconstruction from a set of 2D cross sections, or online data acquisition using a matrix-array transducer, also

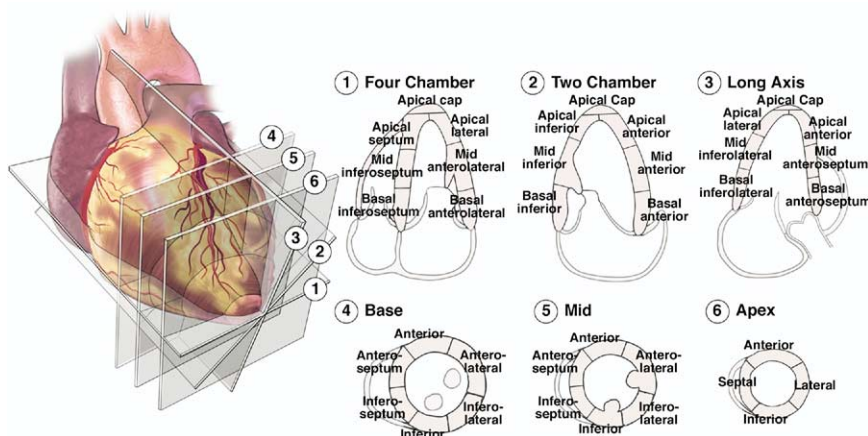


**Figure 8** Segmental analysis of LV walls based on schematic views, in a parasternal short- and long-axis orientation, at 3 different levels. The “apex segments” are usually visualized from apical 4-chamber, apical 2 and 3-chamber views. The apical cap can only be appreciated on some contrast studies. A 16-segment model can be used, without the apical cap, as described in an ASE 1989 document.<sup>2</sup> A 17-segment model, including the apical cap, has been suggested by the American Heart Association Writing Group on Myocardial Segmentation and Registration for Cardiac Imaging.<sup>62</sup>

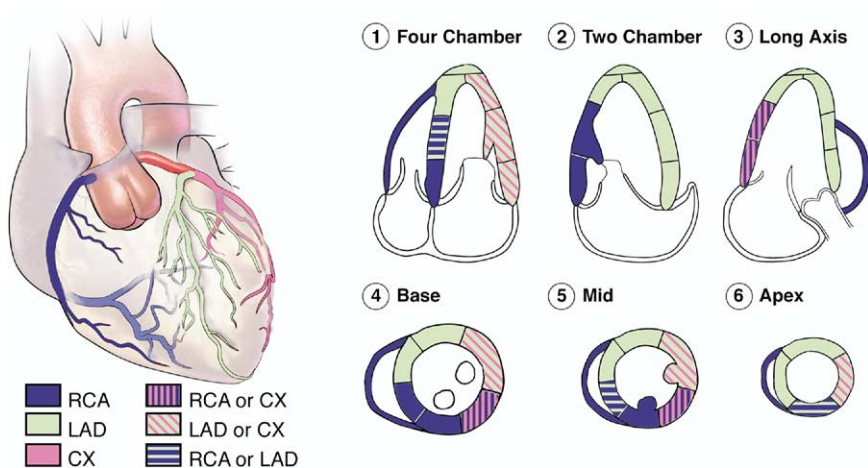


**Figure 9** Typical distributions of the right coronary artery (RCA), the left anterior descending (LAD), and the circumflex (CX) coronary arteries. The arterial distribution varies between patients. Some segments have variable coronary perfusion.

known as real-time 3D echocardiography. After acquisition of the raw data, calculation of LV volumes and mass requires identification of endocardial borders (and for mass epicardial border) using manual or semiautomated algorithms. These borders are then processed to calculate the cavity or myocardial volume by summation of disks<sup>54,56</sup> or other methods.<sup>46-48</sup>

Regardless of which acquisition or analysis method is used, 3D echocardiography does not rely on geometric assumptions for volume/mass calculations and is not subject to plane positioning errors, which can lead to chamber foreshortening. Studies comparing 3D echocardiographic LV volumes

or mass with other gold standards (eg, MRI) have confirmed 3D echocardiography to be accurate. Compared with magnetic resonance data, LV and right ventricular (RV) volumes calculated from 3D echocardiography showed significantly better agreement (smaller bias), lower scatter, and lower intraobserver and interobserver variability than 2D echocardiography.<sup>46,54,57,60</sup> The superiority of 3D echocardiographic LV mass calculations over values calculated from M-mode or 2D echocardiography has been convincingly shown.<sup>55,57,59</sup> RV volume and mass have also been measured by 3D echocardiography with good agreement with magnetic resonance data.<sup>58,61</sup> Current limitations include the require-

ment of regular rhythm, relative inferior image quality of real-time 3D echocardiography compared with 2D images, and the time necessary for offline data analysis. However, the greater number of acquired data points, the lack of geometric assumptions, increasingly sophisticated 3D image, and measurements solutions offset these limitations.

### Regional LV Function

In 1989, the ASE recommended a 16-segment model for LV segmentation.<sup>2</sup> This model consists of 6 segments at both basal and midventricular levels and 4 segments at the apex (Figure 8). The attachment of the RV wall to the LV defines the septum, which is divided at basal and mid-LV levels into anteroseptum and inferoseptum. Continuing counterclockwise, the remaining segments at both basal and midventricular levels are labeled as inferior, inferolateral, anterolateral, and anterior. The apex includes septal, inferior, lateral, and anterior segments. This model has become widely used in echocardiography. In contrast, nuclear perfusion imaging, cardiovascular magnetic resonance, and cardiac computed tomography have commonly used a larger number of segments.

In 2002, the American Heart Association Writing Group on Myocardial Segmentation and Registration for Cardiac Imaging, in an attempt to establish segmentation standards applicable to all types of imaging, recommended a 17-segment model (Figure 8).<sup>62</sup> This differs from the previous 16-segment model predominantly by the addition of a 17th segment, the apical cap. The apical cap is the segment beyond the end of the LV cavity. Refinements in echocardiographic imaging, including harmonics and contrast imaging, are believed to permit improved imaging of the apex. Either model is practical for clinical application yet sufficiently detailed for semiquantitative analysis. The 17-segment model should be predominantly used for myocardial perfusion studies or any time efforts are made to compare between imaging modalities. The 16-segment model is appropriate for studies assessing wall-motion abnormalities, as the tip of the normal apex (segment 17) does not move.

The mass and size of the myocardium as assessed at autopsy is the basis for determining the distribution of segments. Sectioned into basal, midventricular, and apical thirds, perpendicular to the LV long axis, with the midventricular third defined by the papillary muscles, the measured myocardial mass in adults without cardiac disease was 43% for the base, 36% for the midcavity, and 21% for the apex.<sup>63</sup> The 16-segment model closely approximates this, creating a distribution of 37.5% for both the basal and midportions and 25% for the apical portion. The 17-segment model creates a distribution of 35.3%, 35.3%, and 29.4% for the basal, mid, and apical

portions (including the apical cap) of the heart, respectively.

Variability exists in the coronary artery blood supply to myocardial segments. Nevertheless, the segments are usually attributed to the 3 major coronary arteries are shown in the TTE distributions of Figure 9.<sup>62</sup>

Since the 1970s, echocardiography has been used for the evaluation of LV regional wall motion during infarction and ischemia.<sup>64-66</sup> It is recognized that regional myocardial blood flow and regional LV systolic function are related over a wide range of blood flows.<sup>67</sup> Although regional wall-motion abnormalities at rest may not be seen until the luminal diameter stenosis exceeds 85%, with exercise, a coronary lesion of 50% can result in regional dysfunction. It is recognized that echocardiography can overestimate the amount of ischemic or infarcted myocardium, as wall motion of adjacent regions may be affected by tethering, disturbance of regional loading conditions, and stunning.<sup>68</sup> Therefore, wall thickening and motion should be considered. Moreover, it should be remembered that regional wall-motion abnormalities may occur in the absence of coronary artery disease.

It is recommended that each segment be analyzed individually and scored on the basis of its motion and systolic thickening. Ideally, the function of each segment should be confirmed in multiple views. Segment scores are as follows: normal or hyperkinesis = 1, hypokinesis = 2, akinesis (negligible thickening) = 3, dyskinesis (paradoxical systolic motion) = 4, and aneurysmal (diastolic deformation) = 5.<sup>1</sup> Wall-motion score index can be derived as a sum of all scores divided by the number of segments visualized.

### Assessment of LV Remodeling and the Use of Echocardiography in Clinical Trials

LV remodeling describes the process by which the heart changes its size, geometry, and function over time. Quantitative 2D TTE enables characterization of LV remodeling that occurs in healthy individuals and in a variety of heart diseases. LV remodeling may be physiologic when the heart increases in size but maintains normal function during growth, physical training, and pregnancy. Several studies have demonstrated that both isometric and isotonic exercise cause remodeling of the LV and RV chamber sizes and wall thicknesses.<sup>69-73</sup> These changes in highly trained, elite athlete hearts are directly related to the type and duration of exercise and have been characterized echocardiographically. With isometric exercise, a disproportionate increase occurs in LV mass compared with the increase in LV diastolic volume, resulting in significantly greater wall thickness to cavity size ratio (h/R ratio) than takes place in healthy nonathletic individuals with no change in ejection phase indices of LV contractile func-



tion.<sup>69-73</sup> This physiologic hypertrophic remodeling of the athlete heart is reversible with cessation of endurance training and is related to the total increase in lean body weight,<sup>70</sup> and triggered by enhanced cardiac sympathetic activity.<sup>74</sup> Remodeling may be compensatory in chronic pressure overload because of systemic hypertension or aortic stenosis resulting in concentric hypertrophy (increased wall thickness, normal cavity volume, and preserved EF) (Figure 5). Compensatory LV remodeling also occurs in chronic volume overload associated with mitral or aortic regurgitation, which induces a ventricular architecture characterized by eccentric hypertrophy, LV chamber dilatation, and initially normal contractile function. Pressure and volume overload may remain compensated by appropriate hypertrophy, which normalizes wall stress such that hemodynamics and EF remain stable during the long term. However, in some patients, chronically increased afterload cannot be normalized indefinitely and the remodeling process becomes pathologic.

Transition to pathologic remodeling is heralded by progressive ventricular dilatation, distortion of cavity shape, and disruption of the normal geometry of the mitral annulus and subvalvular apparatus resulting in mitral regurgitation. The additional volume load from mitral regurgitation escalates the deterioration in systolic function and development of heart failure. LV dilatation begets mitral regurgitation and mitral regurgitation begets further LV dilatation, progressive remodeling, and contractile dysfunction.

Changes in LV size and geometry caused by hypertension (Figure 5) reflect the dominant underlying hemodynamic alterations associated with blood pressure elevation.<sup>22,75</sup> The pressure overload pattern of concentric hypertrophy is uncommon in otherwise healthy individuals with hypertension and is associated with high systolic blood pressure and high peripheral resistance. In contrast, eccentric LV hypertrophy is associated with normal peripheral resistance but high cardiac index consistent with excess circulating blood volume. Concentric remodeling (normal LV mass with increased RWT) is characterized by high peripheral resistance, low cardiac index, and increased arterial stiffness.<sup>76,77</sup>

A unique form of remodeling occurs after MI as a result of the abrupt loss of contracting myocytes.<sup>22,78</sup> Early expansion of the infarct zone is associated with early LV dilatation as the increased regional wall stress is redistributed to preserve stroke volume. The extent of early and late postinfarction remodeling is determined by a number of factors, including size and location of infarction, activation of the sympathetic nervous system, and up-regulation of the renin/angiotensin/aldosterone system and natriuretic peptides. Between a half and

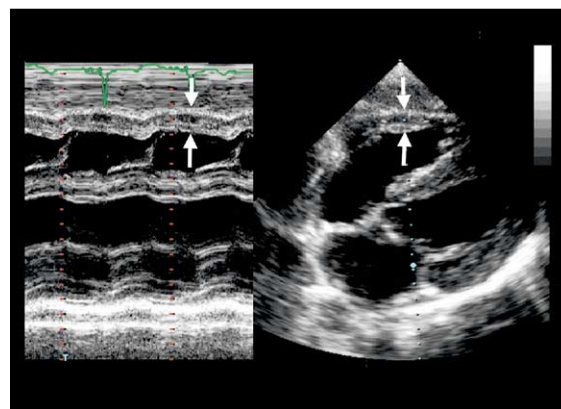


**Figure 10** Methods of measuring right ventricular wall thickness (arrows) from M-mode (left) and subcostal trans-thoracic (right) echocardiograms.

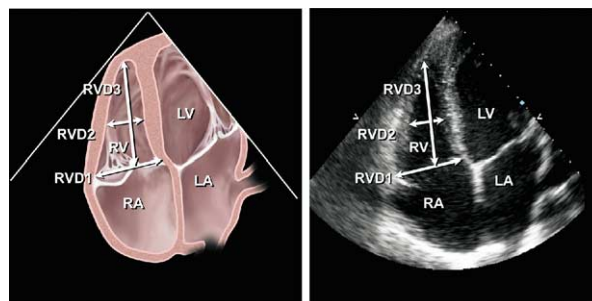


**Figure 11** Midright ventricular diameter measured in apical 4-chamber view at level of left ventricular papillary muscles.

a third of patients postinfarction experience progressive dilatation<sup>79,80</sup> with distortion of ventricular geometry and secondary mitral regurgitation. Mitral regurgitation further increases the propensity for deterioration in LV function and development of congestive heart failure. Pathologic LV remodeling is the final common pathway to heart failure, whether the initial stimulus is chronic pressure, chronic volume overload, genetically determined cardiomyopathy, or MI. The cause of LV dysfunction in approximately two thirds of the 4.9 million patients with heart failure in the United States is coronary artery disease.<sup>81</sup>

Although LV remodeling in patients with chronic systemic hypertension, chronic valvular regurgitation, and primary cardiomyopathies has been described, the transition to heart failure is less well known because the time course is so prolonged. By contrast, the time course from MI to heart failure is shorter and has been clearly documented.

The traditional quantitative echocardiographic measurements recommended for the evaluation of LV remodeling included estimates of LV volumes either



**Table 7** Reference limits and partition values of right ventricular and pulmonary artery size

	Reference range	Mildly abnormal	Moderately abnormal	Severely abnormal
RV dimensions (Figure 12)				
Basal RV diameter (RVD 1), cm	2.0–2.8	2.9–3.3	3.4–3.8	≥3.9
Mid-RV diameter (RVD 2), cm	2.7–3.3	3.4–3.7	3.8–4.1	≥4.2
Base-to-apex length (RVD 3), cm	7.1–7.9	8.0–8.5	8.6–9.1	≥9.2
RVOT diameters (Figure 13, 14)				
Above aortic valve (RVOT 1), cm	2.5–2.9	3.0–3.2	3.3–3.5	≥3.6
Above pulmonic valve (RVOT 2), cm	1.7–2.3	2.4–2.7	2.8–3.1	≥3.2
PA diameter				
Below pulmonic valve (PA 1), cm	1.5–2.1	2.2–2.5	2.6–2.9	≥3.0

RV, Right ventricular; RVOT, right ventricular outflow tract; PA, pulmonary artery.  
Data from Foale et al.<sup>76</sup>

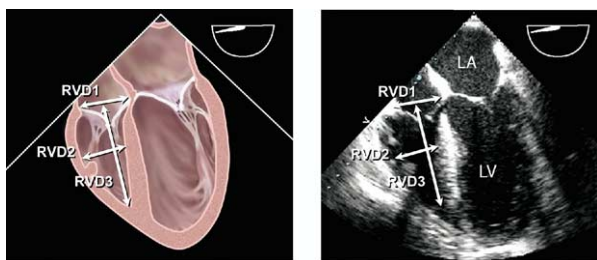


**Figure 12** Transesophageal echocardiographic measurements of right ventricular (RV) diameters from midesophageal 4-chamber view, best imaged after optimizing maximum obtainable RV size by varying angles from approximately 0 to 20 degrees.

from biplane or single plane images as advocated by the ASE. Although biplane and single plane volume estimations are not interchangeable, both estimates are equally sensitive for detecting time-dependent LV remodeling and deteriorating contractile function.<sup>77</sup> LV volumes and derived EF have been demonstrated to predict adverse cardiovascular events at follow-up, including death, recurrent infarction, heart failure, ventricular arrhythmias, and mitral regurgitation in numerous postinfarction and heart failure trials.<sup>78-81</sup>

This committee recommends the use of quantitative estimation of LV volumes, LV EF, LV mass, and shape as described in the respective sections above to follow LV remodeling induced by physiologic and pathologic stimuli. In addition, these measurements provide prognostic information incremental to that of baseline clinical demographics.

#### QUANTIFICATION OF THE RV AND RV OUTFLOW TRACT

The normal RV is a complex crescent-shaped structure wrapped around the LV and is incompletely visualized in any single 2D echocardiographic view. Thus, accurate assessment of RV

**Table 8** Reference limits and partition values of right ventricular size and function as measured in the apical 4-chamber view

	Reference range	Mildly abnormal	Moderately abnormal	Severely abnormal
RV diastolic area, cm <sup>2</sup>	11–28	29–32	33–37	≥38
RV systolic area, cm <sup>2</sup>	7.5–16	17–19	20–22	≥23
RV fractional area change, %	32–60	25–31	18–24	≤17

RV, Right ventricular.  
Data from Weyman.<sup>80</sup>

morphology and function requires integration of multiple echocardiographic views, including parasternal long- and short-axis, RV inflow, apical 4-chamber, and subcostal. Although multiple methods for quantitative echocardiographic RV assessment have been described, in clinical practice assessment of RV structure and function remains mostly qualitative. Nevertheless, numerous studies have recently emphasized the importance of RV function in the prognosis of a variety of cardiopulmonary diseases suggesting that more routine quantification of RV function is warranted under most clinical circumstances.

Compared with the LV, the RV is a thin-walled structure under normal conditions. The normal RV is accustomed to a low pulmonary resistance and, hence, low afterload; thus, normal RV pressure is low and RV compliance high. The RV is, therefore, sensitive to changes in afterload, and alterations in RV size and function are indicators of increased pulmonary vascular resistance and load transmitted from the left-sided chambers. Elevations in RV afterload in adults are manifested acutely by RV dilatation and chronically by concentric RV hypertrophy. In addition, intrinsic RV abnormalities, such as infarction or RV dysplasia<sup>82</sup> can cause RV dilatation or reduced RV wall thick-

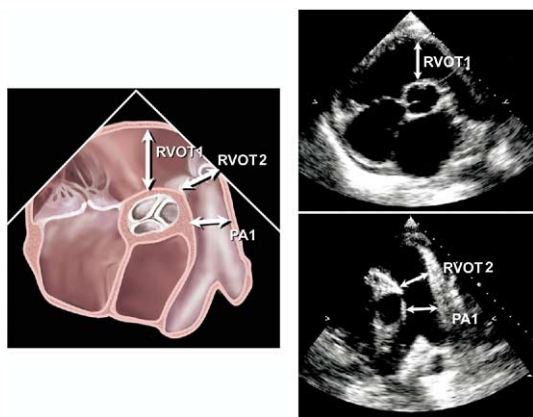


**Figure 13** Measurement of right ventricular outflow tract diameter at subpulmonary region (*RVOT1*) and pulmonic valve annulus (*RVOT2*) in midesophageal aortic valve short-axis view, using multiplane angle of approximately 45 to 70 degrees.

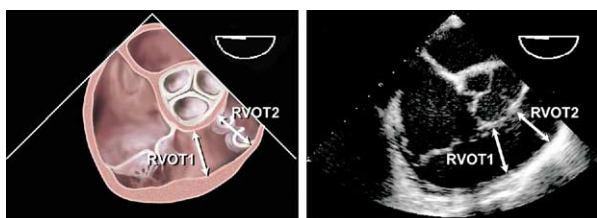


**Figure 14** Measurement of right ventricular outflow tract at pulmonic valve annulus (*RVOT2*) and main pulmonary artery from parasternal short-axis view.

ness. Thus, assessment of RV size and wall thickness is integral to the assessment of RV function.

RV free wall thickness, normally less than 0.5 cm, is measured using either M-mode or 2D imaging. Although RV free wall thickness can be assessed from the apical and parasternal long-axis views, the subcostal view measured at the peak of the R wave at the level of the tricuspid valve chordae tendinae provides less variation and closely correlates with RV peak systolic pressure (Figure 10).<sup>75</sup> Care must be taken to avoid over-measurement because of the presence of epicardial fat deposition and coarse trabeculations within the RV.

Qualitative assessment of RV size is easily accomplished from the apical 4-chamber view (Figure 11). In this view, RV area or midcavity diameter should be smaller than that of the LV. In cases of moderate enlargement, the RV cavity area is similar to that of the LV and it may share the apex of the heart. As RV dilation progresses, the cavity area will exceed that of the LV and the RV will be apex forming. Quantitative assessment of RV size is also best performed in the apical 4-chamber

view. Care must be taken to obtain a true nonfore-shortened apical-4 chamber view, oriented to obtain the maximum RV dimension, before making these measurements. Measurement of the mid-cavity and basal RV diameter in the apical 4-chamber view at end diastole is a simple method to quantify RV size (Figure 11). In addition, RV longitudinal diameter can be measured from this view. Table 7 provides normal RV dimensions from the apical 4-chamber view.<sup>76,80,83</sup>

RV size may be assessed with TEE in the midesophageal 4-chamber view (Figure 12). Midesophageal 4-chamber view, which generally parallels what is obtainable from the apical 4-chamber view, should originate at the mid-LA level and pass through the LV apex with the multiplane angle adjusted to maximize the tricuspid annulus diameter—usually between 10 and 20 degrees.

RV systolic function is generally estimated qualitatively in clinical practice. When the evaluation is based on a qualitative assessment, the displacement of the tricuspid annulus should be observed. In systole, the tricuspid annulus will normally descend toward the apex 1.5 to 2.0 cm. Tricuspid annular excursion of less than 1.5 cm has been associated with poor prognosis in a variety of cardiovascular diseases.<sup>84</sup> Although a number of techniques exist for accurate quantitation, direct calculation of RV volumes and EF remains problematic given the complex geometry of the RV and the lack of standard methods for assessing RV volumes. Nevertheless, a number of echocardiographic techniques may be used to assess RV function. RV fractional area change measured in the apical 4-chamber view is a simple method for assessment of RV function that has correlated with RV EF measured by MRI ( $r = 0.88$ ) and has been related to outcome in a number of disease states.<sup>81,85</sup> Normal RV areas and fractional area change are shown in Table 8. Additional assessment of the RV systolic function includes tissue imaging of tricuspid annular velocity or RV index of myocardial performance (Tei index).<sup>86</sup>

RV outflow tract (RVOT) extends from the anterosuperior aspect of the RV to the pulmonary artery, and includes the pulmonary valve. It is best imaged from the parasternal long-axis view angled superiorly, and the parasternal short axis at the base of the heart. It can also be imaged from the subcostal long and transverse windows and the apical window. Measurement of the RVOT is most accurate from the parasternal short axis (Figure 13) just proximal to the pulmonary valve. Mean RVOT measurements are shown in Table 7.<sup>75</sup> With TEE, the midesophageal RV inflow-outflow view usually provides the best image of the RVOT just proximal to the pulmonary valve (Figure 14).

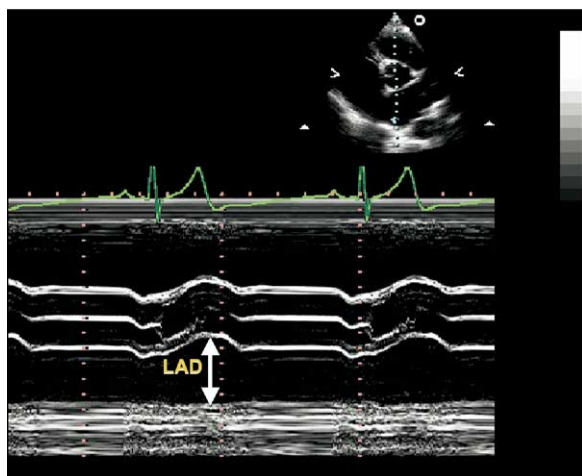
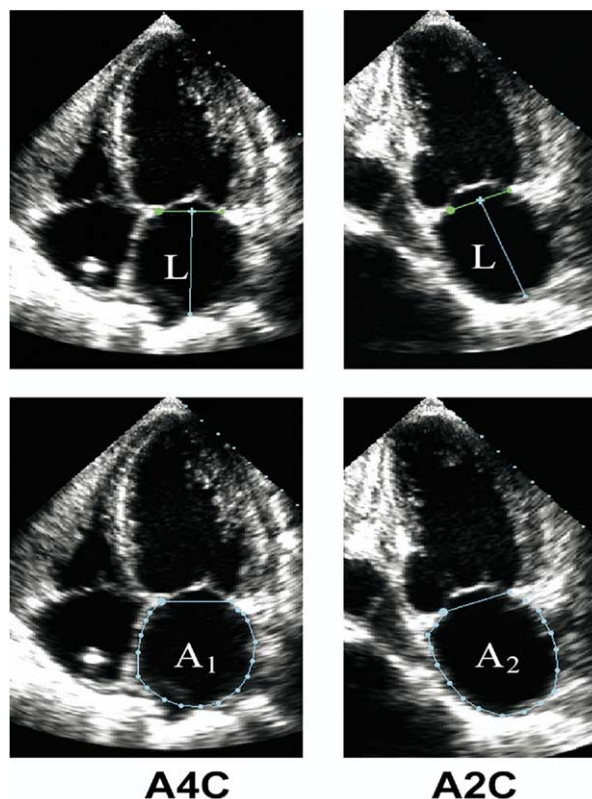


**Figure 15** Measurement of left atrial diameter (*LAD*) from M-mode, guided by parasternal short-axis image (*upper right*) at level of aortic valve. Linear method is not recommended.

#### QUANTIFICATION OF LEFT ATRIAL AND RIGHT ATRIAL SIZE

The LA fulfills 3 major physiologic roles that impact on LV filling and performance. The LA acts as a contractile pump that delivers 15% to 30% of the LV filling, as a reservoir that collects pulmonary venous return during ventricular systole, and as a conduit for the passage of stored blood from the LA to the LV during early ventricular diastole.<sup>87</sup> Increased LA size is associated with adverse cardiovascular outcomes.<sup>88-90</sup> An increase in atrial size most commonly is related to increased wall tension as a result of increased filling pressure.<sup>91,92</sup> Although increased filling volumes can cause an increase in LA size, the adverse outcomes associated with increased dimension and volume are more strongly associated with increased filling pressure. Relationships exist between increased LA size and the incidence of atrial fibrillation and stroke,<sup>93-101</sup> risk of overall mortality after MI,<sup>102,103</sup> and risk of death and hospitalization in patients with dilated cardiomyopathy.<sup>104-108</sup> LA enlargement is a marker of both the severity and chronicity of diastolic dysfunction and magnitude of LA pressure elevation.<sup>88,91,92</sup>

The LA size is measured at the end-ventricular systole when the LA chamber is at its greatest dimension. While recording images for computing LA volume, care should be taken to avoid foreshortening of the LA. The base of the LA should be at its largest size indicating that the imaging plane passes through the maximal short-axis area. The LA length should also be maximized ensuring alignment along the true long axis of the LA. When performing



A4C

A2C

$$\text{Left Atrial Volume} = \frac{8}{3}\pi[(A_1)(A_2)/(L)]^*$$

\* (L) is the shortest of either the A4C or A2C length

**Figure 16** Measurement of left atrial (LA) volume from area-length (*L*) method using apical 4-chamber (*A4C*) and apical 2-chamber (*A2C*) views at ventricular end systole (maximum LA size). *L* is measured from back wall to line across hinge points of mitral valve. Shorter *L* from either A4C or A2C is used in equation.

planimetry, the LA, the confluences of the pulmonary veins, and LA appendage should be excluded.

With TEE, the LA frequently cannot fit in its entirety into the image sector. Measurements of LA volume from this approach cannot be reliably performed; however, LA dimension can be estimated combining measurements from different imaging planes.

#### LA Linear Dimension

The LA can be visualized from multiple echocardiographic views from which several potential LA dimensions can be measured. However, the large volume of prior clinical and research work used



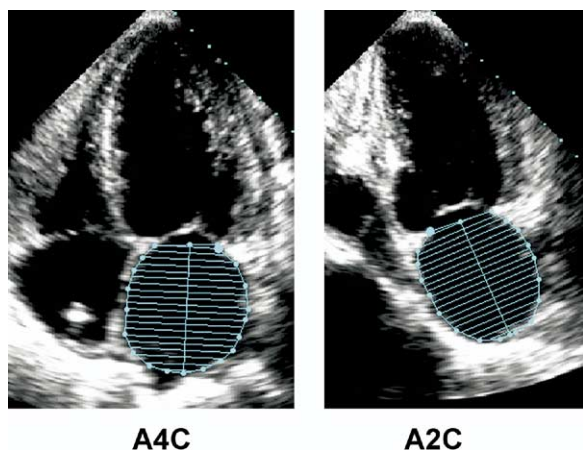


**Figure 17** Measurement of left atrial (LA) volume from biplane method of disks (modified Simpson's rule) using apical 4-chamber (A4C) and apical 2-chamber (A2C) views at ventricular end systole (maximum LA size).

M-mode or 2D anteroposterior (AP) linear dimension obtained from the parasternal long-axis view, making this the standard for linear LA measurement (Figure 15).<sup>93,95,96,98,104,105</sup> The convention for M-mode measurement is to measure from the leading edge of the posterior aortic wall to the leading edge of the posterior LA wall. However, to avoid the variable extent of space between the LA and aortic root, the trailing edge of the posterior aortic is recommended.

Although these linear measurements have been shown to correlate with angiographic measurements and have been widely used in clinical practice and research, they inaccurately represent true LA size.<sup>109,110</sup> Evaluation of the LA in the AP dimension assumes that a consistent relationship is maintained between the AP dimension and all other LA dimensions as the atrium enlarges, which is often not the case.<sup>111,112</sup> Expansion of the LA in the AP dimension may be constrained by the thoracic cavity between the sternum and the spine. Predominant enlargement in the superior-inferior and medial-lateral dimensions will alter LA geometry such that the AP dimension may not be representative of LA size. For these reasons, AP linear dimensions of the LA as the sole measure of LA size may be misleading and should be accompanied by LA volume determination in both clinical practice and research.

### LA Volume Measurements

When LA size is measured in clinical practice, volume determinations are preferred over linear dimensions because they allow accurate assessment of the asymmetric remodeling of the LA chamber.<sup>111</sup> In addition, the strength of the relationship between cardiovascular disease is stronger for LA volume than for LA linear dimensions.<sup>97,113</sup> Echocardiographic

measures of LA volume have been compared with cinemagnetic tomography, biplane contrast ventriculography, and MRI.<sup>109,114-116</sup> These studies have shown either good agreement or a tendency for echocardiographic measurements to underestimate comparative LA volumes.

The simplest method for estimating LA volume is the cube formula, which assumes that the LA volume is that of a sphere with a diameter equal to the LA AP dimension. However, this method has proven to be inferior to other volume techniques.<sup>109,111,117</sup> LA volumes are best calculated using either an ellipsoid model or Simpson's rule.<sup>88,89,97,101,102,109-111,115-117</sup>

The ellipsoid model assumes that the LA can be adequately represented as a prolate ellipse with a volume of  $4\pi/3 (L/2) (D_1/2) (D_2/2)$ , where L is the long axis (ellipsoid) and  $D_1$  and  $D_2$  are orthogonal short-axis dimensions. LA volume can be estimated using this biplane dimension-length formula by substituting the LA AP diameter acquired from the parasternal long axis as  $D_1$ , LA medial-lateral dimension from the parasternal short-axis as  $D_2$ , and the LA long-axis from the apical 4-chamber for L.<sup>117-119</sup> Simplified methods using nonorthogonal linear measurements for estimation of LA volume have been proposed.<sup>113</sup> Volume determined using linear dimensions is very dependent on careful selection of the location and direction of the minor-axis dimensions and has been shown to significantly underestimate LA volume.<sup>117</sup>

To estimate the LA minor-axis dimension of the ellipsoid more reliably, the long-axis LA areas can be traced and a composite dimension derived. This dimension takes into account the entire LA border, rather than a single linear measurement. When long-axis area is substituted for minor-axis dimension, the biplane area-length formula is used:  $8 (A_1) (A_2)/3\pi (L)$ , where  $A_1$  and  $A_2$  represent the maximal planimetered LA area acquired from the apical 4- and 2-chamber views, respectively, and L is length. The length remains the LA long-axis length determined as the distance of the perpendicular line measured from the middle of the plane of the mitral annulus to the superior aspect of the LA (Figure 16). In the area-length formula the length is measured in both the 4- and 2-chamber views and the shortest of these 2 length measurements is used in the formula.

The area-length formula can be computed from a single plane, typically the apical 4-chamber, by assuming  $A_1 = A_2$  such that volume =  $8 (A_1)^2/3\pi (L)$  (Figure 16).<sup>120</sup> However, this method makes geometric assumptions that may be inaccurate. In older individuals the diaphragm lifts the cardiac apex upward, which increases the angle between ventricle and atrium. Thus, the apical 4-chamber view will commonly intersect the atria tangentially in older individuals and result in underestimation of volume using a single plane technique. Because the



**Table 9** Reference limits and partition values for left atrial dimensions/volumes

	Women				Men			
	Reference range	Mildly abnormal	Moderately abnormal	Severely abnormal	Reference range	Mildly abnormal	Moderately abnormal	Severely abnormal
Atrial dimensions								
LA diameter, cm	2.7–3.8	3.9–4.2	4.3–4.6	≥4.7	3.0–4.0	4.1–4.6	4.7–5.2	≥5.2
LA diameter/BSA, cm/m <sup>2</sup>	1.5–2.3	2.4–2.6	2.7–2.9	≥3.0	1.5–2.3	2.4–2.6	2.7–2.9	≥3.0
RA minor-axis dimension, cm	2.9–4.5	4.6–4.9	5.0–5.4	≥5.5	2.9–4.5	4.6–4.9	5.0–5.4	≥5.5
RA minor-axis dimension/BSA, cm/m <sup>2</sup>	1.7–2.5	2.6–2.8	2.9–3.1	≥3.2	1.7–2.5	2.6–2.8	2.9–3.1	≥3.2
Atrial area								
LA area, cm <sup>2</sup>	≤20	20–30	30–40	>40	≤20	20–30	30–40	>40
Atrial volumes								
LA volume, mL	22–52	53–62	63–72	≥73	18–58	59–68	69–78	≥79
<i>LA volume/BSA, mL/m<sup>2</sup></i>	<i>22 ± 6</i>	<i>29–33</i>	<i>34–39</i>	<i>≥40</i>	<i>22 ± 6</i>	<i>29–33</i>	<i>34–39</i>	<i>≥40</i>

BSA, Body surface area; LA, left atrial; RA, right atrial.  
Bold italic values: Recommended and best validated.

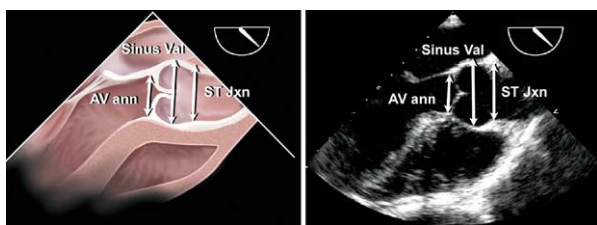


**Figure 18** Measurement of aortic root diameters at aortic valve annulus (*AV ann*) level, sinuses of Valsalva (*Sinus Val*), and sinotubular junction (*ST Jxn*) from midesophageal long-axis view of aortic valve, usually at angle of approximately 110 to 150 degrees. Annulus is measured by convention at base of aortic leaflets. Although leading edge to leading edge technique is demonstrated for the Sinus Val and ST Jxn, some prefer inner edge to inner edge method. (See text for further discussion.)

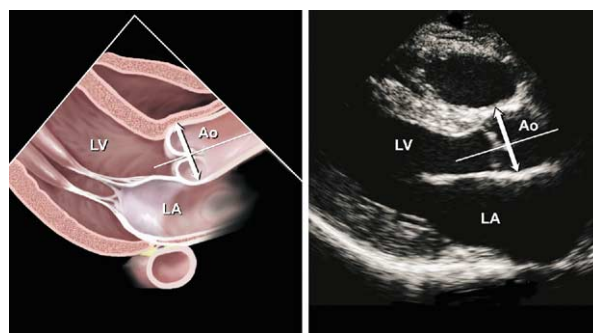


**Figure 19** Measurement of aortic root diameter at sinuses of Valsalva from 2-dimensional parasternal long-axis image. Although leading edge to leading edge technique is shown, some prefer inner edge to inner edge method. (See text for further discussion.)

majority of prior research and clinical studies have used the biplane area-length formula, it is the recommended ellipsoid method (Figures 15 and 16).

LA volume may also be measured using Simpson's rule, similar to its application for LV measurements, which states that the volume of a geometric figure can be calculated from the sum of the volumes of smaller figures of similar shape. Most commonly, Simpson's algorithm divides the LA into a series of stacked oval disks whose height is *h* and whose orthogonal minor and major axes are *D*<sub>1</sub> and *D*<sub>2</sub> (method of disks). The volume of the entire LA can be derived from the sum of the volume of the individual disks. Volume =  $\pi/4 (h) \sum (D_1) (D_2)$ . The formula is integrated with the aid of a computer and the calculated volume provided by the software package online (Figure 17).

The use of the Simpson's method in this way requires the input of biplane LA planimetry to derive the diameters. Optimal contours should be obtained orthogonally around the long axis of the LA using

TTE apical views. Care should be taken to exclude the pulmonary veins from the LA tracing. The inferior border should be represented by the plane of the mitral annulus. A single plane method of disks could be used to estimate LA volume by assuming the stacked disks are circular  $V = \pi/4 (h) \sum (D_1)^2$ .<sup>2</sup> However, as noted above, this makes the assumption that the LA width in the apical 2- and 4-chamber are identical, which is often not the case and, therefore, this formula is not preferred.

Three-dimensional echocardiography should provide the most accurate evaluation of LA volume and has shown promise; however, to date no consensus exists on the specific method that should be used for data acquisition and there is no comparison with established normal values.<sup>121-125</sup>

#### Normal Values of LA Measurements

The nonindexed LA linear measurements are taken from a Framingham Heart Study cohort of 1099 participants between the ages of 20 and 45 years

who were not obese, of average height, and without cardiovascular disease (Table 9).<sup>11</sup> Slightly higher values have been reported in a cohort of 767 participants without cardiovascular disease in which obesity and height were not exclusion criteria.<sup>113</sup> Both body size and aging have been noted to influence LA size.<sup>10,87,113</sup> There are also sex differences in LA size; however, these are nearly completely accounted for by variation in body size.<sup>87,113,120,124</sup> The influence of body size on LA size is typically corrected by indexing to some measure of body size. In fact, from childhood onward the indexed atrial volume changes very little.<sup>125</sup> Several indexing methods have been proposed, such as height, weight, estimated lean body mass, and BSA.<sup>10,113</sup> The most commonly used convention, and that recommended by this committee, is indexing LA size by dividing by BSA.

Normal indexed LA volume has been determined using the preferred biplane techniques (area-length or method of disks) in a number of studies involving several hundred patients to be  $22 \pm 6$  cc/m<sup>2</sup>.<sup>88,120,126,127</sup> Absolute LA volume has also been reported; however, in clinical practice indexing to BSA accounts for variations in body size and should, therefore, be used. As cardiac risk and LA size are closely linked, more importantly than simply characterizing the degree of LA enlargement, normal reference values for LA volume allow prediction of cardiac risk. There are now multiple peer-reviewed articles that validate the progressive increase in risk associated with having LA volumes greater than these normative values.<sup>89,97,99-103,106-108,128</sup> Consequently, indexed LA volume measurements should become a routine laboratory measure because they reflect the burden and chronicity of elevated LV filling pressure and are a strong predictor of outcome.

### Right Atrium

Much less research and clinical data are available on quantifying right atrial (RA) size. Although the RA can be assessed from many different views, quantification of RA size is most commonly performed from the apical 4-chamber view. The minor-axis dimension should be taken in a plane perpendicular to the long axis of the RA and extends from the lateral border of the RA to the interatrial septum. Normative values for the RA minor axis are shown in Table 9.<sup>80,129</sup> Although RA dimension may vary by sex, no separate male and female reference values can be recommended at this time.

Although limited data are available for RA volumes, assessment of RA volumes would be more robust and accurate for determination of RA size than linear dimensions. As there are no standard orthogonal RA views to use an apical biplane calculation, the single plane area-length and method of

disks formulas have been applied to RA volume determination in several small studies.<sup>120,130,131</sup> We believe there is too little peer-reviewed validated literature to recommend normal RA volumetric values at this time. However, limited data on a small number of healthy individuals revealed that indexed RA volumes are similar to LA normal values in men (21 mL/m<sup>2</sup>) but appear to be slightly smaller in women.<sup>120</sup>

---

## QUANTIFICATION OF THE AORTA AND INFERIOR VENA CAVA

---

### Aortic Measurements

Recordings should be made from the parasternal long-axis acoustic window to visualize the aortic root and proximal ascending aorta. Two-dimensional images should be used to visualize the LV outflow tract and the aortic root should be recorded in different views in varying intercostal spaces and at different distances from the left sternal border. Right parasternal views, recorded with the patient in a right lateral decubitus position, are also useful. Measurements are usually taken at: (1) aortic valve annulus (hinge point of aortic leaflets); (2) the maximal diameter in the sinuses of Valsalva; and (3) sinotubular junction (transition between the sinuses of Valsalva and the tubular portion of the ascending aorta).

Views used for measurement should be those that show the largest diameter of the aortic root. When measuring the aortic diameter, it is particularly important to use the maximum diameter measured perpendicular to the long axis of the vessel in that view. Some experts favor inner edge to inner edge techniques to match those used by other methods of imaging the aorta, such as MRI and computed tomography scanning. However, the normative data for echocardiography were obtained using the leading edge technique (Figure 18). Advances in ultrasound instrumentation that have resulted in improved image resolution should minimize the difference between these measurement methods.

Two-dimensional aortic diameter measurements are preferable to M-mode measurements, as cyclic motion of the heart and resultant changes in M-mode cursor location relative to the maximum diameter of the sinuses of Valsalva result in systematic underestimation (by ~2 mm) of aortic diameter by M-mode in comparison with the 2D aortic diameter.<sup>132</sup> The aortic annular diameter is measured between the hinge points of the aortic valve leaflets (inner edge-inner edge) in the parasternal or apical long-axis views that reveal the largest aortic annular diameter with color flow mapping to clarify tissue-blood interfaces if necessary.<sup>132</sup>

The thoracic aorta can be better imaged using TEE than TTE, as most of it is in the near field of the

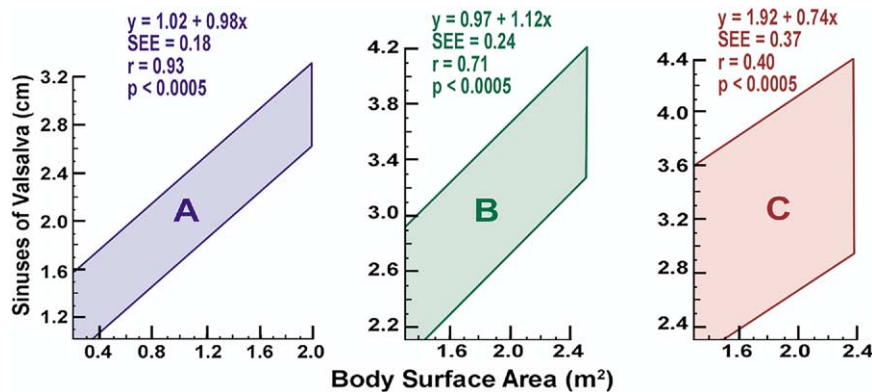


**Figure 20** The 95% confidence intervals for aortic root diameter at sinuses of Valsalva based on body surface area in children and adolescents (A), adults aged 20 to 39 years (B), and adults aged 40 years or older (C). (Reprinted from American Journal of Cardiology, Volume 64, Roman et al., Two-dimensional echocardiographic aortic root dimensions in normal children and adults, 507-12, 1989, with permission from Excerpta Medica, Inc.)

transducer. The ascending aorta can be seen in long axis using the midesophageal aortic valve long-axis view at about 130 degrees and the midesophageal ascending aorta long-axis view. The short-axis view of the ascending aorta is obtained using the midesophageal views at about 45 degrees. For measurements of the descending aorta, short-axis views at about 0 degrees, and long-axis views at about 90 degrees, can be recorded from the level of the diaphragm up to the aortic arch (Figure 19). The arch itself and origins of two of the great vessels can be seen in most patients. There is a blind spot in the upper ascending aorta and the proximal arch that is not seen by TEE because of the interposed tracheal bifurcation.

#### Identification of Aortic Root Dilatation

Aortic root diameter at the sinuses of Valsalva is related most strongly to BSA and age. Therefore, BSA may be used to predict aortic root diameter in 3 age strata: younger than 20 years, 20 to 40 years, and older than 40 years, by published equations.<sup>132</sup> Aortic root dilatation at the sinuses of Valsalva is defined as an aortic root diameter above the upper limit of the 95% confidence interval of the distribution in a large reference population.<sup>132</sup> Aortic dilatation can be easily detected by plotting observed aortic root diameter versus BSA on previously published nomograms (Figure 20).<sup>132</sup> Equations to determine the expected aortic diameter at the sinuses of Valsalva in relation to body surface area for each of the 3 age strata are found in Figure 20. The aortic root index, or ratio of observed to expected aortic root diameter, can be calculated by dividing the observed diameter by the expected diameter. Aortic dilatation is strongly associated with the presence and progression of aortic regurgitation<sup>133</sup> and with the occurrence of aortic dissection.<sup>134</sup> The presence

of hypertension appears to have minimal impact on aortic root diameter at the sinuses of Valsalva,<sup>133,135</sup> but is associated with enlargement of more distal aortic segments.

#### Evaluation of the Inferior Vena Cava

Examination of the inferior vena cava (IVC) from the subcostal view should be included as part of the routine TTE examination. It is generally agreed that the diameter of the IVC should be measured with the patient in the left decubitus position at 1.0 to 2.0 cm from the junction with the RA, using the long-axis view. For accuracy, this measurement should be made perpendicular to the IVC long axis. The diameter of the IVC decreases in response to inspiration when the negative intrathoracic pressure leads to an increase in RV filling from the systemic veins. The diameter of the IVC and the percent decrease in the diameter during inspiration correlate with RA pressure. The relationship has been called the collapsibility index.<sup>136</sup> Evaluation of the inspiratory response often requires a brief sniff, as normal inspiration may not elicit this response.

The normal IVC diameter is less than 1.7 cm. There is a 50% decrease in the diameter when the RA pressure is normal (0-5 mm Hg). A dilated IVC (>1.7 cm) with normal inspiratory collapse ( $\geq 50\%$ ) is suggestive of a mildly elevated RA pressure (6-10 mm Hg). When the inspiratory collapse is less than 50%, the RA pressure is usually between 10 and 15 mm Hg. Finally, a dilated IVC without any collapse suggests a markedly increased RA pressure of greater than 15 mm Hg. In contrast, a small IVC (usually <1.2 cm) with spontaneous collapse often is seen in the presence of intravascular volume depletion.<sup>137</sup>

There are several additional conditions to be considered in evaluating the IVC. Athletes have been

shown to have dilated IVCs with normal collapsibility index. Studies<sup>137,138</sup> have found that the mean IVC diameter in athletes was  $2.31 \pm .46$  compared with  $1.14 \pm 0.13$  in aged-matched control subjects. The highest diameters were seen in highly trained swimmers.

One study showed that a dilated IVC in the mechanically ventilated patient did not always indicate a high RA pressure. However, a small IVC (<1.2 cm) had a 100% specificity for a RA pressure of less than 10 mm Hg with a low sensitivity.<sup>139</sup> A more recent study suggested that there was a better correlation when the IVC diameter was measured at end expiration and end diastole using M-mode echocardiography.<sup>140</sup>

The use of the IVC size and dynamics is encouraged for estimation of RA pressure. This estimate should be used in estimation of the pulmonary artery pressure based on the tricuspid regurgitant jet velocity.

The authors wish to thank Harvey Feigenbaum, MD, and Nelson B. Schiller for their careful review and thoughtful comments.

## REFERENCES

1. Sahn DJ, DeMaria A, Kisslo J, Weyman A. Recommendations regarding quantitation in M-mode echocardiography: results of a survey of echocardiographic measurements. *Circulation* 1978;58:1072-83.
2. Schiller NB, Shah PM, Crawford M, DeMaria A, Devereux R, Feigenbaum H, et al. Recommendations for quantitation of the left ventricle by two-dimensional echocardiography: American Society of Echocardiography committee on standards, subcommittee on quantitation of two-dimensional echocardiograms. *J Am Soc Echocardiogr* 1989;2:358-67.
3. Hirata K, Watanabe H, Beppu S, Muro T, Teragaki M, Yoshiyama M, et al. Pitfalls of echocardiographic measurement in tissue harmonic imaging: in vitro and in vivo study. *J Am Soc Echocardiogr* 2002;15:1038-44.
4. McGavigan AD, Dunn FG, Goodfield NE. Secondary harmonic imaging overestimates left ventricular mass compared to fundamental echocardiography. *Eur J Echocardiogr* 2003; 4:178-81.
5. Feigenbaum H, Armstrong W, Ryan T. Feigenbaum's echocardiography. 6th ed. Philadelphia: Lippincott, Williams and Wilkins; 2005.
6. Mulvagh SL, DeMaria AN, Feinstein SB, Burns PN, Kaul S, Miller JG, et al. Contrast echocardiography: current and future applications. *J Am Soc Echocardiogr* 2000;13:331-42.
7. Nahar T, Croft L, Shapiro R, Fruchtman S, Diamond J, Henzlava M, et al. Comparison of four echocardiographic techniques for measuring left ventricular ejection fraction. *Am J Cardiol* 2000;86:1358-62.
8. Colombo PC, Municino A, Brofferio A, Kholdarova L, Nanna M, Ilercil A, et al. Cross-sectional multiplane transesophageal echocardiographic measurements: comparison with standard transthoracic values obtained in the same setting. *Echocardiography* 2002;19:383-90.
9. Hozumi T, Shakudo M, Shah PM. Quantitation of left ventricular volumes and ejection fraction by biplane transesophageal echocardiography. *Am J Cardiol* 1993;72:356-9.
10. Vasan RS, Levy D, Larson MG, Benjamin EJ. Interpretation of echocardiographic measurements: a call for standardization. *Am Heart J* 2000;139:412-22.
11. Vasan RS, Larson MG, Levy D, Evans JC, Benjamin EJ. Distribution and categorization of echocardiographic measurements in relation to reference limits: the Framingham heart study; formulation of a height- and sex-specific classification and its prospective validation. *Circulation* 1997;96:1863-73.
12. Devereux RB, Roman MJ. Evaluation of cardiac and vascular structure by echocardiography and other noninvasive techniques. In: Laragh JH, Brenner BM, editors. Hypertension: pathophysiology, diagnosis, treatment. 2nd ed. New York: Raven Press; 1995. p. 1969-85.
13. Gottdiener JS, Bednarz J, Devereux R, Gardin J, Klein A, Manning WJ, et al. American Society of Echocardiography recommendations for use of echocardiography in clinical trials. *J Am Soc Echocardiogr* 2004;17:1086-119.
14. Wyatt HL, Heng MK, Meerbaum S, Hestenes JD, Cobo JM, Davidson RM, et al. Cross-sectional echocardiography, I: analysis of mathematic models for quantifying mass of the left ventricle in dogs. *Circulation* 1979;60:1104-13.
15. Reichek N, Helak J, Plappert T, Sutton MS, Weber KT. Anatomic validation of left ventricular mass estimates from clinical two-dimensional echocardiography: initial results. *Circulation* 1983;67:348-52.
16. Helak JW, Reichek N. Quantitation of human left ventricular mass and volume by two-dimensional echocardiography: in vitro anatomic validation. *Circulation* 1981;63:1398-407.
17. Schiller NB, Skioldebrand CG, Schiller EJ, Mavroudis CC, Silverman NH, Rahimtoola SH, et al. Canine left ventricular mass estimation by two-dimensional echocardiography. *Circulation* 1983;68:210-6.
18. Triulzi MO, Gillam LD, Gentile F, Newell J, Weyman A. Normal adult cross-sectional echocardiographic values: linear dimensions and chamber areas. *Echocardiography* 1984; 1:403-26.
19. Devereux RB, Wachtell K, Gerds E, Boman K, Nieminen MS, Papademetriou V, et al. Prognostic significance of left ventricular mass change during treatment of hypertension. *JAMA* 2004;292:1-7.
20. Ilercil A, O'Grady MJ, Roman MJ, Paranicas M, Lee ET, Welty TK, et al. Reference values for echocardiographic measurements in urban and rural populations of differing ethnicity: the strong heart study. *J Am Soc Echocardiogr* 2001;14:601-11.
21. Devereux RB, Alonso DR, Lutas EM, Gottlieb GJ, Campo E, Sachs I, et al. Echocardiographic assessment of left ventricular hypertrophy: comparison to necropsy findings. *Am J Cardiol* 1986;57:450-8.
22. Ganau A, Devereux RB, Roman MJ, de Simone G, Pickering TG, Saba PS, et al. Patterns of left ventricular hypertrophy and geometric remodeling in essential hypertension. *J Am Coll Cardiol* 1992;19:1550-8.
23. Devereux RB, de Simone G, Pickering TG, Schwartz JE, Roman MJ. Relation of left ventricular midwall function to cardiovascular risk factors and arterial structure and function. *Hypertension* 1998;31:929-36.
24. Palmieri V, Dahlof B, DeQuattro V, Sharpe N, Bella JN, de Simone G, et al. Reliability of echocardiographic assessment of left ventricular structure and function: the PRESERVE



- study; prospective randomized study evaluating regression of ventricular enlargement. *J Am Coll Cardiol* 1999;34:1625-32.
25. Nidorf SM, Picard MH, Triulzi MO, Thomas JD, Newell J, King ME, et al. New perspectives in the assessment of cardiac chamber dimensions during development and adulthood. *J Am Coll Cardiol* 1992;19:983-8.
  26. Pearlman JD, Triulzi MO, King ME, Newell J, Weyman AE. Limits of normal left ventricular dimensions in growth and development: analysis of dimensions and variance in the two-dimensional echocardiograms of 268 normal healthy subjects. *J Am Coll Cardiol* 1988;12:1432-41.
  27. Lang RM, Borow KM, Neumann A, Janzen D. Systemic vascular resistance: an unreliable index of left ventricular afterload. *Circulation* 1986;74:1114-23.
  28. Quinones MA, Waggoner AD, Reduto LA, Nelson JG, Young JB, Winters WL Jr, et al. A new, simplified and accurate method for determining ejection fraction with two-dimensional echocardiography. *Circulation* 1981;64:744-53.
  29. Teichholz LE, Kreulen T, Herman MV, Gorlin R. Problems in echocardiographic volume determinations: echocardiographic-angiographic correlations in the presence of absence of asynergy. *Am J Cardiol* 1976;37:7-11.
  30. de Simone G, Devereux RB, Roman MJ, Ganau A, Saba PS, Alderman MH, et al. Assessment of left ventricular function by the midwall fractional shortening/end-systolic stress relation in human hypertension. *J Am Coll Cardiol* 1994;23:1444-51.
  31. Shimizu G, Zile MR, Blaustein AS, Gaasch WH. Left ventricular chamber filling and midwall fiber lengthening in patients with left ventricular hypertrophy: overestimation of fiber velocities by conventional midwall measurements. *Circulation* 1985;71:266-72.
  32. Celentano A, Palmieri V, Arezzi E, Mureddu GF, Sabatella M, Di MG, et al. Gender differences in left ventricular chamber and midwall systolic function in normotensive and hypertensive adults. *J Hypertens* 2003;21:1415-23.
  33. Gerds E, Zabalgoitia M, Bjornstad H, Svendsen TL, Devereux RB. Gender differences in systolic left ventricular function in hypertensive patients with electrocardiographic left ventricular hypertrophy (the LIFE study). *Am J Cardiol* 2001;87:980-3.
  34. Devereux RB, Roman MJ, de Simone G, O'Grady MJ, Paranicas M, Yeh JL, et al. Relations of left ventricular mass to demographic and hemodynamic variables in American Indians: the strong heart study. *Circulation* 1997;96:1416-23.
  35. Devereux RB, Bella JN, Palmieri V, Oberman A, Kitzman DW, Hopkins PN, et al. Left ventricular systolic dysfunction in a biracial sample of hypertensive adults: the hypertension genetic epidemiology network (HyperGEN) study. *Hypertension* 2001;38:417-23.
  36. Roman MJ, Pickering TG, Schwartz JE, Pini R, Devereux RB. Association of carotid atherosclerosis and left ventricular hypertrophy. *J Am Coll Cardiol* 1995;25:83-90.
  37. Wahr DW, Wang YS, Schiller NB. Left ventricular volumes determined by two-dimensional echocardiography in a normal adult population. *J Am Coll Cardiol* 1983;1:863-8.
  38. de Simone G, Daniels SR, Devereux RB, Meyer RA, Roman MJ, de Divitiis O, et al. Left ventricular mass and body size in normotensive children and adults: assessment of allometric relations and impact of overweight. *J Am Coll Cardiol* 1992;20:1251-60.
  39. Devereux RB, Palmieri V, Sharpe N, De Quattro V, Bella JN, de Simone G, et al. Effects of once-daily angiotensin-converting enzyme inhibition and calcium channel blockade-based antihypertensive treatment regimens on left ventricular hypertrophy and diastolic filling in hypertension: the prospective randomized enalapril study evaluating regression of ventricular enlargement (preserve) trial. *Circulation* 2001;104:1248-54.
  40. Kizer JR, Arnett DK, Bella JN, Paranicas M, Rao DC, Province MA, et al. Differences in left ventricular structure between black and white hypertensive adults: the hypertension genetic epidemiology network study. *Hypertension* 2004;43:1182-8.
  41. Devereux RB, Casale PN, Kligfield P, Eisenberg RR, Miller D, Campo E, et al. Performance of primary and derived M-mode echocardiographic measurements for detection of left ventricular hypertrophy in necropsied subjects and in patients with systemic hypertension, mitral regurgitation and dilated cardiomyopathy. *Am J Cardiol* 1986;57:1388-93.
  42. Malcolm DD, Burns TL, Mahoney LT, Lauer RM. Factors affecting left ventricular mass in childhood: the Muscatine study. *Pediatrics* 1993;92:703-9.
  43. Daniels SR, Meyer RA, Liang YC, Bove KE. Echocardiographically determined left ventricular mass index in normal children, adolescents and young adults. *J Am Coll Cardiol* 1988;12:703-8.
  44. Daniels SR, Kimball TR, Morrison JA, Khoury P, Meyer RA. Indexing left ventricular mass to account for differences in body size in children and adolescents without cardiovascular disease. *Am J Cardiol* 1995;76:699-701.
  45. de SG, Devereux RB, Daniels SR, Koren MJ, Meyer RA, Laragh JH. Effect of growth on variability of left ventricular mass: assessment of allometric signals in adults and children and their capacity to predict cardiovascular risk. *J Am Coll Cardiol* 1995;25:1056-62.
  46. Gopal AS, Keller AM, Rigling R, King DL Jr, King DL. Left ventricular volume and endocardial surface area by three-dimensional echocardiography: comparison with two-dimensional echocardiography and nuclear magnetic resonance imaging in normal subjects. *J Am Coll Cardiol* 1993;22:258-70.
  47. Handschumacher MD, Lethor JP, Siu SC, Mele D, Rivera JM, Picard MH, et al. A new integrated system for three-dimensional echocardiographic reconstruction: development and validation for ventricular volume with application in human subjects. *J Am Coll Cardiol* 1993;21:743-53.
  48. Jiang L, Vazquez de Prada JA, Handschumacher MD, Vuille C, Guerro JL, Picard MH, et al. Quantitative three-dimensional reconstruction of aneurysmal left ventricles: in vitro and in vivo validation. *Circulation* 1995;91:222-30.
  49. King DL, Harrison MR, King DL Jr, Gopal AS, Martin RP, DeMaria AN. Improved reproducibility of left atrial and left ventricular measurements by guided three-dimensional echocardiography. *J Am Coll Cardiol* 1992;20:1238-45.
  50. Kuhl HP, Franke A, Frielingsdorf J, Flaskamp C, Krebs W, Flachskampf FA, et al. Determination of left ventricular mass and circumferential wall thickness by three-dimensional reconstruction: in vitro validation of a new method that uses a multiplane transesophageal transducer. *J Am Soc Echocardiogr* 1997;10:107-19.
  51. Roelandt JR, Ten Cate FJ, Vletter WB, Taams MA. Ultrasonic dynamic three-dimensional visualization of the heart with a multiplane transesophageal imaging transducer. *J Am Soc Echocardiogr* 1994;7:217-29.
  52. Sheikh K, Smith SW, von Ramm O, Kisslo J. Real-time, three-dimensional echocardiography: feasibility and initial use. *Echocardiography* 1991;8:119-25.

53. Wollschlager H, Zeiher AM, Geibel A, Kasper W, Just H, Wollschlager S. Transesophageal echo computer tomography: computational reconstruction of any desired view of the beating heart. In: Hanrath P, Uebis R, Krebs W, editors. Cardiovascular imaging by ultrasound. Dordrecht: Kluwer; 1993.
54. Buck T, Hunold P, Wentz KU, Tkalec W, Nesser HJ, Erbel R. Tomographic three-dimensional echocardiographic determination of chamber size and systolic function in patients with left ventricular aneurysm: comparison to magnetic resonance imaging, cineventriculography, and two-dimensional echocardiography. *Circulation* 1997;96:4286-97.
55. Kuhl HP, Franke A, Merx M, Hoffmann R, Puschmann D, Hanrath P. Rapid quantification of left ventricular function and mass using transesophageal three-dimensional echocardiography: validation of a method that uses long-axis cut-planes. *Eur J Echocardiogr* 2000;1:213-21.
56. Nosir YF, Fioretti PM, Vletter WB, Boersma E, Salustri A, Postma JT, et al. Accurate measurement of left ventricular ejection fraction by three-dimensional echocardiography: a comparison with radionuclide angiography. *Circulation* 1996;94:460-6.
57. Gopal AS, Schnellbaecher MJ, Shen Z, Boxt LM, Katz J, King DL. Freehand three-dimensional echocardiography for determination of left ventricular volume and mass in patients with abnormal ventricles: comparison with magnetic resonance imaging. *J Am Soc Echocardiogr* 1997;10:853-61.
58. Shiota T, Jones M, Chikada M, Fleishman CE, Castellucci JB, Cotter B, et al. Real-time three-dimensional echocardiography for determining right ventricular stroke volume in an animal model of chronic right ventricular volume overload. *Circulation* 1998;97:1897-900.
59. Mor-Avi V, Sugeng L, Weinert L, MacEneaney P, Caiani EG, Koch R, et al. Fast measurement of left ventricular mass with real-time three-dimensional echocardiography: comparison with magnetic resonance imaging. *Circulation* 2004;110:1814-8.
60. Jiang L, Siu SC, Handschumacher MD, Luis GJ, Vazquez de Prada JA, King ME, et al. Three-dimensional echocardiography: in vivo validation for right ventricular volume and function. *Circulation* 1994;89:2342-50.
61. Jiang L, Vazquez de Prada JA, Handschumacher MD, Guerro JL, Vlahakes GJ, King ME, et al. Three-dimensional echocardiography: in vivo validation for right ventricular free wall mass as an index of hypertrophy. *J Am Coll Cardiol* 1994;23:1715-22.
62. Cerqueira MD, Weissman NJ, Dilsizian V, Jacobs AK, Kaul S, Laskey WK, et al. Standardized myocardial segmentation and nomenclature for tomographic imaging of the heart: a statement for healthcare professionals from the cardiac imaging committee of the council on clinical cardiology of the American Heart Association. *Circulation* 2002;105:539-42.
63. Edwards WD, Tajik AJ, Seward JB. Standardized nomenclature and anatomic basis for regional tomographic analysis of the heart. *Mayo Clin Proc* 1981;56:479-97.
64. Heger JJ, Weyman AE, Wann LS, Dillon JC, Feigenbaum H. Cross-sectional echocardiography in acute myocardial infarction: detection and localization of regional left ventricular asynergy. *Circulation* 1979;60:531-8.
65. Kerber RE, Abboud FM. Echocardiographic detection of regional myocardial infarction: an experimental study. *Circulation* 1973;47:997-1005.
66. Weiss JL, Bulkley BH, Hutchins GM, Mason SJ. Two-dimensional echocardiographic recognition of myocardial injury in man: comparison with postmortem studies. *Circulation* 1981;63:401-8.
67. Ross J Jr. Myocardial perfusion-contraction matching: implications for coronary heart disease and hibernation. *Circulation* 1991;83:1076-83.
68. Lieberman AN, Weiss JL, Jugdutt BI, Becker LC, Bulkley BH, Garrison JG, et al. Two-dimensional echocardiography and infarct size: relationship of regional wall motion and thickening to the extent of myocardial infarction in the dog. *Circulation* 1981;63:739-46.
69. Fagard R, Aubert A, Lysens R, Staessen J, Vanhees L, Amery A. Noninvasive assessment of seasonal variations in cardiac structure and function in cyclists. *Circulation* 1983;67:896-901.
70. Fisher AG, Adams TD, Yanowitz FG, Ridges JD, Orsmond G, Nelson AG. Noninvasive evaluation of world-class athletes engaged in different modes of training. *Am J Cardiol* 1989;63:337-41.
71. Vos M, Hauser AM, Dressendorfer RH, Hashimoto T, Dudlets P, Gordon S, et al. Enlargement of the right heart in the endurance athlete: a two-dimensional echocardiographic study. *Int J Sports Med* 1985;6:271-5.
72. Douglas PS, O'Toole ML, Hiller WD, Reichek N. Left ventricular structure and function by echocardiography in ultraendurance athletes. *Am J Cardiol* 1986;58:805-9.
73. Pelliccia A, Maron BJ, Spataro A, Proschan MA, Spirito P. The upper limit of physiologic cardiac hypertrophy in highly trained elite athletes. *N Engl J Med* 1991;324:295-301.
74. Neri Serneri GG, Boddi M, Modesti PA, Cecioni I, Coppo M, Padeletti L, et al. Increased cardiac sympathetic activity and insulin-like growth factor-I formation are associated with physiological hypertrophy in athletes. *Circ Res* 2001;89:977-82.
75. Matsukubo H, Matsuura T, Endo N, Asayama J, Watanabe T. Echocardiographic measurement of right ventricular wall thickness: a new application of subxiphoid echocardiography. *Circulation* 1977;56:278-84.
76. Foale R, Nihoyannopoulos P, McKenna W, Kleinebenne A, Nadazdin A, Rowland E, et al. Echocardiographic measurement of the normal adult right ventricle. *Br Heart J* 1986;56:33-44.
77. Roman MJ, Ganau A, Saba PS, Pini R, Pickering TG, Devereux RB. Impact of arterial stiffening on left ventricular structure. *Hypertension* 2000;36:489-94.
78. Picard MH, Wilkins GT, Ray PA, Weyman AE. Natural history of left ventricular size and function after acute myocardial infarction: assessment and prediction by echocardiographic endocardial surface mapping. *Circulation* 1990;82:484-94.
79. St John Sutton M, Pfeffer MA, Moye L, Plappert T, Rouleau JL, Lamas G, et al. Cardiovascular death and left ventricular remodeling two years after myocardial infarction: baseline predictors and impact of long-term use of captopril; information from the survival and ventricular enlargement (SAVE) trial. *Circulation* 1997;96:3294-9.
80. Weyman A. Practices and principles of echocardiography. 2nd ed. Philadelphia: Lippincott, Williams and Wilkins; 1994.
81. Zornoff LA, Skali H, Pfeffer MA, St John SM, Rouleau JL, Lamas GA, et al. Right ventricular dysfunction and risk of heart failure and mortality after myocardial infarction. *J Am Coll Cardiol* 2002;39:1450-5.
82. Yoerger DM, Marcus F, Sherrill D, Calkins H, Towbin JA, Zareba W, et al. Echocardiographic findings in patients

- meeting task force criteria for arrhythmogenic right ventricular dysplasia: new insights from the multidisciplinary study of right ventricular dysplasia. *J Am Coll Cardiol* 2005; 45: 860-5.
83. Schenk P, Globits S, Koller J, Brunner C, Artemiou O, Klepetko W, et al. Accuracy of echocardiographic right ventricular parameters in patients with different end-stage lung diseases prior to lung transplantation. *J Heart Lung Transplant* 2000;19:145-54.
  84. Samad BA, Alam M, Jensen-Urstad K. Prognostic impact of right ventricular involvement as assessed by tricuspid annular motion in patients with acute myocardial infarction. *Am J Cardiol* 2002;90:778-81.
  85. Maslow AD, Regan MM, Panzica P, Heindel S, Mashikian J, Comunale ME. Precardiopulmonary bypass right ventricular function is associated with poor outcome after coronary artery bypass grafting in patients with severe left ventricular systolic dysfunction. *Anesth Analg* 2002;95:1507-18.
  86. Severino S, Caso P, Cicala S, Galderisi M, De Simone L, D'Andrea A, et al. Involvement of right ventricle in left ventricular hypertrophic cardiomyopathy: analysis by pulsed Doppler tissue imaging. *Eur J Echocardiogr* 2000;1:281-8.
  87. Spencer KT, Mor-Avi V, Gorcsan J III, DeMaria AN, Kimball TR, Monaghan MJ, et al. Effects of aging on left atrial reservoir, conduit, and booster pump function: a multi-institution acoustic quantification study. *Heart* 2001;85: 272-7.
  88. Tsang TS, Barnes ME, Gersh BJ, Bailey KR, Seward JB. Left atrial volume as a morphophysiological expression of left ventricular diastolic dysfunction and relation to cardiovascular risk burden. *Am J Cardiol* 2002;90:1284-9.
  89. Tsang TS, Barnes ME, Gersh BJ, Takemoto Y, Rosales AG, Bailey KR, et al. Prediction of risk for first age-related cardiovascular events in an elderly population: the incremental value of echocardiography. *J Am Coll Cardiol* 2003;42: 1199-205.
  90. Kizer JR, Bella JN, Palmieri V, et al. Left atrial diameter as an independent predictor of first clinical cardiovascular events in middle-aged and elderly adults: the strong heart study. *Am Heart J* In press 2005.
  91. Simek CL, Feldman MD, Haber HL, Wu CC, Jayaweera AR, Kaul S. Relationship between left ventricular wall thickness and left atrial size: comparison with other measures of diastolic function. *J Am Soc Echocardiogr* 1995;8:37-47.
  92. Appleton CP, Galloway JM, Gonzalez MS, Gaballa M, Basnight MA. Estimation of left ventricular filling pressures using two-dimensional and Doppler echocardiography in adult patients with cardiac disease: additional value of analyzing left atrial size, left atrial ejection fraction and the difference in duration of pulmonary venous and mitral flow velocity at atrial contraction. *J Am Coll Cardiol* 1993;22: 1972-82.
  93. Benjamin EJ, D'Agostino RB, Belanger AJ, Wolf PA, Levy D. Left atrial size and the risk of stroke and death: the Framingham heart study. *Circulation* 1995;92:835-41.
  94. Bolca O, Akdemir O, Eren M, Dagdeviren B, Yildirim A, Tezel T. Left atrial maximum volume is a recurrence predictor in lone atrial fibrillation: an acoustic quantification study. *Jpn Heart J* 2002;43:241-8.
  95. Di Tullio MR, Sacco RL, Sciacca RR, Homma S. Left atrial size and the risk of ischemic stroke in an ethnically mixed population. *Stroke* 1999;30:2019-24.
  96. Flaker GC, Fletcher KA, Rothbart RM, Halperin JL, Hart RG. Clinical and echocardiographic features of intermittent atrial fibrillation that predict recurrent atrial fibrillation: stroke prevention in atrial fibrillation (SPAF) investigators. *Am J Cardiol* 1995;76:355-8.
  97. Tsang TS, Barnes ME, Bailey KR, Leibson CL, Montgomery SC, Takemoto Y, et al. Left atrial volume: important risk marker of incident atrial fibrillation in 1655 older men and women. *Mayo Clin Proc* 2001;76:467-75.
  98. Vaziri SM, Larson MG, Benjamin EJ, Levy D. Echocardiographic predictors of nonrheumatic atrial fibrillation: the Framingham heart study. *Circulation* 1994;89:724-30.
  99. Barnes ME, Miyasaka Y, Seward JB, Gersh BJ, Rosales AG, Bailey KR, et al. Left atrial volume in the prediction of first ischemic stroke in an elderly cohort without atrial fibrillation. *Mayo Clin Proc* 2004;79:1008-14.
  100. Tsang TS, Barnes ME, Gersh BJ, Bailey KR, Seward JB. Risks for atrial fibrillation and congestive heart failure in patients  $\geq 65$  years of age with abnormal left ventricular diastolic relaxation. *Am J Cardiol* 2004;93:54-8.
  101. Tsang TS, Gersh BJ, Appleton CP, Tajik AJ, Barnes ME, Bailey KR, et al. Left ventricular diastolic dysfunction as a predictor of the first diagnosed nonvalvular atrial fibrillation in 840 elderly men and women. *J Am Coll Cardiol* 2002;40: 1636-44.
  102. Moller JE, Hillis GS, Oh JK, Seward JB, Reeder GS, Wright RS, et al. Left atrial volume: a powerful predictor of survival after acute myocardial infarction. *Circulation* 2003;107:2207-12.
  103. Beinart R, Boyko V, Schwammenthal E, Kuperstein R, Sagie A, Hod H, et al. Long-term prognostic significance of left atrial volume in acute myocardial infarction. *J Am Coll Cardiol* 2004;44:327-34.
  104. Modena MG, Muia N, Sgura FA, Molinari R, Castella A, Rossi R. Left atrial size is the major predictor of cardiac death and overall clinical outcome in patients with dilated cardiomyopathy: a long-term follow-up study. *Clin Cardiol* 1997; 20:553-60.
  105. Quinones MA, Greenberg BH, Kopelen HA, Koilpillai C, Limacher MC, Shindler DM, et al. Echocardiographic predictors of clinical outcome in patients with left ventricular dysfunction enrolled in the SOLVD registry and trials: significance of left ventricular hypertrophy: studies of left ventricular dysfunction. *J Am Coll Cardiol* 2000;35:1237-44.
  106. Rossi A, Cicoira M, Zanolla L, Sandrini R, Golia G, Zardini P, et al. Determinants and prognostic value of left atrial volume in patients with dilated cardiomyopathy. *J Am Coll Cardiol* 2002;40:1425.
  107. Dini FL, Cortigiani L, Baldini U, Boni A, Nuti R, Barsotti L, et al. Prognostic value of left atrial enlargement in patients with idiopathic dilated cardiomyopathy and ischemic cardiomyopathy. *Am J Cardiol* 2002;89:518-23.
  108. Sabharwal N, Cemin R, Rajan K, Hickman M, Lahiri A, Senior R. Usefulness of left atrial volume as a predictor of mortality in patients with ischemic cardiomyopathy. *Am J Cardiol* 2004;94:760-3.
  109. Schabelman S, Schiller NB, Silverman NH, Ports TA. Left atrial volume estimation by two-dimensional echocardiography. *Catheter Cardiovasc Diagn* 1981;7:165-78.
  110. Wade MR, Chandraratna PA, Reid CL, Lin SL, Rahimtoola SH. Accuracy of nondirected and directed M-mode echocardiography as an estimate of left atrial size. *Am J Cardiol* 1987;60:1208-11.
  111. Lester SJ, Ryan EW, Schiller NB, Foster E. Best method in clinical practice and in research studies to determine left atrial size. *Am J Cardiol* 1999;84:829-32.

112. Loperfido F, Pennestri F, Digaetano A, Scabbia E, Santarelli P, Mongiardo R, et al. Assessment of left atrial dimensions by cross sectional echocardiography in patients with mitral valve disease. *Br Heart J* 1983;50:570-8.
113. Pritchett AM, Jacobsen SJ, Mahoney DW, Rodeheffer RJ, Bailey KR, Redfield MM. Left atrial volume as an index of left atrial size: a population-based study. *J Am Coll Cardiol* 2003;41:1036-43.
114. Kircher B, Abbott JA, Pau S, Gould RG, Himelman RB, Higgins CB, et al. Left atrial volume determination by bi-plane two-dimensional echocardiography: validation by cine computed tomography. *Am Heart J* 1991;121:864-71.
115. Rodevan O, Bjornerheim R, Ljosland M, Maehle J, Smith HJ, Ihlen H. Left atrial volumes assessed by three- and two-dimensional echocardiography compared to MRI estimates. *Int J Card Imaging* 1999;15:397-410.
116. Vandenberg BF, Weiss RM, Kinzey J, Acker M, Stark CA, Stanford W, et al. Comparison of left atrial volume by two-dimensional echocardiography and cine-computed tomography. *Am J Cardiol* 1995;75:754-7.
117. Khankirawatana B, Khankirawatana S, Porter T. How should left atrial size be reported? Comparative assessment with use of multiple echocardiographic methods. *Am Heart J* 2004; 147:369-74.
118. Hiraishi S, DiSessa TG, Jarmakani JM, Nakanishi T, Isabel-Jones J, Friedman WF. Two-dimensional echocardiographic assessment of left atrial size in children. *Am J Cardiol* 1983; 52:1249-57.
119. Jessurun ER, van Hemel NM, Kelder JC, Defauw JA, Brutel DLR, Ernst JM, et al. The effect of maze operations on atrial volume. *Ann Thorac Surg* 2003;75:51-6.
120. Wang Y, Gutman JM, Heilbron D, Wahr D, Schiller NB. Atrial volume in a normal adult population by two-dimensional echocardiography. *Chest* 1984;86:595-601.
121. Keller AM, Gopal AS, King DL. Left and right atrial volume by freehand three-dimensional echocardiography: in vivo validation using magnetic resonance imaging. *Eur J Echocardiogr* 2000;1:55-65.
122. Khankirawatana B, Khankirawatana S, Lof J, Porter TR. Left atrial volume determination by three-dimensional echocardiography reconstruction: validation and application of a simplified technique. *J Am Soc Echocardiogr* 2002;15: 1051-6.
123. Poutanen T, Ikonen A, Vainio P, Jokinen E, Tikanoja T. Left atrial volume assessed by transthoracic three-dimensional echocardiography and magnetic resonance imaging: dynamic changes during the heart cycle in children. *Heart* 2000;83:537-42.
124. Knutsen KM, Stugaard M, Michelsen S, Otterstad JE. M-mode echocardiographic findings in apparently healthy, non-athletic Norwegians aged 20-70 years: influence of age, sex and body surface area. *J Intern Med* 1989;225:111-5.
125. Pearlman JD, Triulzi MO, King ME, Abascal VM, Newell J, Weyman AE. Left atrial dimensions in growth and development: normal limits for two-dimensional echocardiography. *J Am Coll Cardiol* 1990;16:1168-74.
126. Gutman J, Wang YS, Wahr D, Schiller NB. Normal left atrial function determined by 2-dimensional echocardiography. *Am J Cardiol* 1983;51:336-40.
127. Thomas L, Levett K, Boyd A, Leung DY, Schiller NB, Ross DL. Compensatory changes in atrial volumes with normal aging: is atrial enlargement inevitable? *J Am Coll Cardiol* 2002;40:1630-5.
128. Losi MA, Betocchi S, Aversa M, Lombardi R, Miranda M, D'Alessandro G, et al. Determinants of atrial fibrillation development in patients with hypertrophic cardiomyopathy. *Am J Cardiol* 2004;94:895-900.
129. Schnittger I, Gordon EP, Fitzgerald PJ, Popp RL. Standardized intracardiac measurements of two-dimensional echocardiography. *J Am Coll Cardiol* 1983;2:934-8.
130. DePace NL, Ren JF, Kotler MN, Mintz GS, Kimbiris D, Kalman P. Two-dimensional echocardiographic determination of right atrial emptying volume: a noninvasive index in quantifying the degree of tricuspid regurgitation. *Am J Cardiol* 1983;52:525-9.
131. Kaplan JD, Evans GT Jr, Foster E, Lim D, Schiller NB. Evaluation of electrocardiographic criteria for right atrial enlargement by quantitative two-dimensional echocardiography. *J Am Coll Cardiol* 1994;23:747-52.
132. Roman MJ, Devereux RB, Kramer-Fox R, O'Loughlin J. Two-dimensional echocardiographic aortic root dimensions in normal children and adults. *Am J Cardiol* 1989; 64:507-12.
133. Roman MJ, Devereux RB, Niles NW, Hochreiter C, Kligfield P, Sato N, et al. Aortic root dilatation as a cause of isolated, severe aortic regurgitation: prevalence, clinical and echocardiographic patterns, and relation to left ventricular hypertrophy and function. *Ann Intern Med* 1987;106: 800-7.
134. Morrison D, Devereux R, Roman MJ. Association of aortic root dilation with aortic dissection: a case-control study. *J Am Coll Cardiol* 2003; p 467A (abstr 861-3).
135. Kim M, Roman MJ, Cavallini MC, Schwartz JE, Pickering TG, Devereux RB. Effect of hypertension on aortic root size and prevalence of aortic regurgitation. *Hypertension* 1996; 28:47-52.
136. Moreno FL, Hagan AD, Holmen JR, Pryor TA, Strickland RD, Castle CH. Evaluation of size and dynamics of the inferior vena cava as an index of right-sided cardiac function. *Am J Cardiol* 1984;53:579-85.
137. Kircher BJ, Himelman RB, Schiller NB. Noninvasive estimation of right atrial pressure from the inspiratory collapse of the inferior vena cava. *Am J Cardiol* 1990;66:493-6.
138. Goldhammer E, Mesnick N, Abinader EG, Sagiv M. Dilated inferior vena cava: a common echocardiographic finding in highly trained elite athletes. *J Am Soc Echocardiogr* 1999; 12:988-93.
139. Jue J, Chung W, Schiller NB. Does inferior vena cava size predict right atrial pressures in patients receiving mechanical ventilation? *J Am Soc Echocardiogr* 1992;5: 613-9.
140. Bendjelid K, Romand JA, Walder B, Suter PM, Fournier G. Correlation between measured inferior vena cava diameter and right atrial pressure depends on the echocardiographic method used in patients who are mechanically ventilated. *J Am Soc Echocardiogr* 2002;15:944-9.